UNIVERSITY OF NEW MEXICO
ALBUQUERQUE

ENGINEERING EXPERIMENT STATION

Technical Report EE-46

Radar Terrain Return from the Spherical Earth at Near-Vertical Incidence

by

B. D. Warner

May 1961

This work performed for
Naval Ordnance Test Station
China Lake, California
Contract No. N123 (60530) 18138A

University of New Mexico

Albuquerque

Engineering Experiment Station

Technical Report EE-46

Radar Terrain Return from the Spherical Earth at Near-Vertical Incidence

by

B. D. Warner

May 1961

This work performed for Naval Ordnance Test Station, China Lake, California Contract No. N123(60530)18138A

- - - - - - -

This report is also being submitted as a thesis in partial fulfillment of the requirements for the Degree of Master of Science in Electrical Engineering at the University of New Mexico.

ABSTRACT

A scalar equation for the power returned to a radio altimeter is developed by probability methods to explain the scattering mechanism of the earth's surface at any altitude, including altitudes such that the sphericity of the earth becomes an important factor. The power return equation is resolved into a specular component plus a random or scatter component. The relative maynitudes of these components depend upon the surface roughness of the irradiated target.

An analytic expression for the scattering cross-section is derived on the assumption that the surface may be reasonably described by a normal bivariate probability density function with a Gaussian correlation function. The scattering cross-section is found to be a function of the angle of incidence and the statistics of the rough surface. The result approaches the isotropic scatterer for extremely rough surfaces.

An insignificant error in return power is incurred by neglecting the curvature of the earth's surface at altitudes up to 400 miles. Here the error in the specular component is + 1 db and that in the scatter component is + 0.5 db.

It is not expected that the scattering cross-section will be independent of large changes in altitude in practical applications. The irradiated target area increases as the radar altitude increases, thus changing the statistical information available to the radar.

Table of Contents

CHAPTER I

INTRODUCTION

Since 1955 the University of New Mexico has been carrying on research and experimental data reduction on the scattering of radar return signals from earth at near-vertical incidence. The work to date has considered scattering at radar altitudes of 2,000 to 12,000 feet as a large quantity of data is available from an extensive experiment performed by the Sandia Corporation, Albuquerque, New Mexico.[1] Based on these previous studies, this paper is a theoretical study of radar terrain return at altitudes such that the sphericity of the earth must be considered.

Much has been written about a specular component (or specular highlight) being observed in power returned from scattering surfaces. R. K. Moore has proposed a scalar theory for separating the specular and random components of the field returned from such scattering surfaces.[2] Here his technique has been applied to the high altitude problem.

The definitions for the terms 'specular' and 'scatter' as used in this paper are as follows. A scattering surface is defined as an irregular surface irradiated by the radar. It is

---

1 Reports issued by the organizations involved in this experiment are listed in the Bibliography, Part B.

2 Moore, R. K., 'Resolution of Vertical Incidence Radar Return into Random and Specular Components,' Tech. Report EE-6, Univ of New Mexico Engr. Exp. Stat., July, 1957.

assumed that the autocorrelation function of surface heights is invariant over the irradiated area. The specular signal is phase coherent with the transmitted signal, and is identical, except for magnitude, with the signal that would be received from a perfectly smooth surface. The resolved specular signal from a scattering surface is reduced by a multiplying factor that is a function of the surface roughness and does not fade as the radar antenna moves over the target area. The scatter component of return signal is not phase coherent with the transmitted signal and fades as the antenna moves over the target area.

As the field returned from a scattering surface has been resolved into specular and random components, the power returned will also have specular and random (or scatter) components. Thus, it becomes necessary to obtain an expression for the specular power reflected from a smooth sphere. V. A. Fock has derived the equations for an arbitrary wave front reflected from an arbitrary surface.[3] Here his results are specialized to the case of a spherical wave front reflected from a spherical surface and expressed in terms of power.

A scalar equation describing the manner in which power is reradiated from a rough surface has been derived by Moore and

---

[3] Fock, V. A., "Generalization of the Reflection Formulas to the Case of Reflection of an Arbitrary Wave from a Surface of Arbitrary Form," Zh. eksp. teon. Fiz., Vol. 20, pp.961-978, 1950. Translation available in Astia Document No. AD 117276.

Williams.[4,5] The expression for specular plus scatter power returned to the radar is obtained by combining Moore and Williams equation with Moore's method of resolving the return field into specular and random components. It is shown that as the altitude of the antenna above the surface of the sphere is decreased, the power returned from the rough sphere approaches a previously derived result for the power returned from a rough plane.[6]

Determining the scattering cross-section of a rough surface is one of the more difficult problems of radar terrain return studies. It is here assumed that a normal bivariate probability density function, with a Gaussian correlation function for height versus distance, will reasonably describe a rough surface. This is essentially the approach taken by Davies to describe backscatter from the sea surface.[7] The assumption of a two-dimensional probability density function for surface roughness permits the calculation of an analytic average scattering cross-section per unit area as a function of angle of incidence. The analytic scattering cross-section contains statistical surface

---

[4] Moore, R. K., and Williams, C. S., Jr., "Radar Terrain Return at Near-Vertical Incidence," PROC. I.R.E., Vol. 45 p. 228, 1957.

[5] A similar result has been obtained with a different approach to the problem by Nelson, D., Hagn, G., Rorden, L., and Clark, N., "An Investigation of the Backscatter of High-Frequency Radio Waves from Land, Sea Water, and Ice," Final Report, Contract Nonr 2917 (00), Stanford Research Institute, May, 1960.

[6] Moore, R. K., Op. Cit., Tech. Report, EE-6

[7] Davies, H., "Reflection of Electromagnetic Waves from a Rough Surface," Proc. Instn. Elect. Engrs. (London) Part IV Vol. 101, pp. 209-14, August 1954.

roughness parameters which are difficult to determine numerically for a given target.

The analytic scattering cross-section may be used to predict the average power returned to the radar provided the surface roughness parameters can be determined. By combining the predicted average power with the range of fading for the target, upper and lower bounds can be found for 90% of the individual returned pulses.[8] Several examples of median power return pulses have been calculated and the approximate range of fading is given for the scatter component.

---

[8] Edison, A. R., "Radar Terrain Return Statistics at Near-Vertical Incidence," Tech. Report EE-35, Univ of New Mexico Engr. Exp. Stat., Oct. 1960.

CHAPTER II

RESOLUTION OF THE RETURN FIELD INTO SPECULAR AND SCATTER COMPONENTS

The field strength, F_{ni}, incident upon an area element, ΔA_n, a distance R_n from the source is, within a constant of proportionality,

$$F_{ni} = \frac{e^{-jkR_n}}{R_n} , \qquad (2.1)$$

where k is the wave number. Then the field strength reradiated back to the source by the area element is, within a different constant of proportionality,

$$F_n = \frac{e^{-j2kR_n}}{R_n^2} \Delta A_n . \qquad (2.2)$$

Summing over all area elements,

$$F = \sum_n F_n = \sum_n \frac{e^{-j2kR_n}}{R_n^2} \Delta A_n . \qquad (2.3)$$

The mean surface of the sphere is considered to be covered with scatterers which may or may not be exactly the mean radius distance a from the center of the sphere. The deviation of a scatterer from the mean surface will be denoted by δ_n, and the radar range to that scatterer by R_n in contrast to R_{on} for the radar range to the mean spherical surface as shown in Figure 2.1.

Applying the law of cosines to the triangle R_{on}, R_n, δ_n,

$$R_n^2 = R_{on}^2 + \delta_n^2 - 2\delta_n R_{on} \cos\theta_i . \qquad (2.4)$$

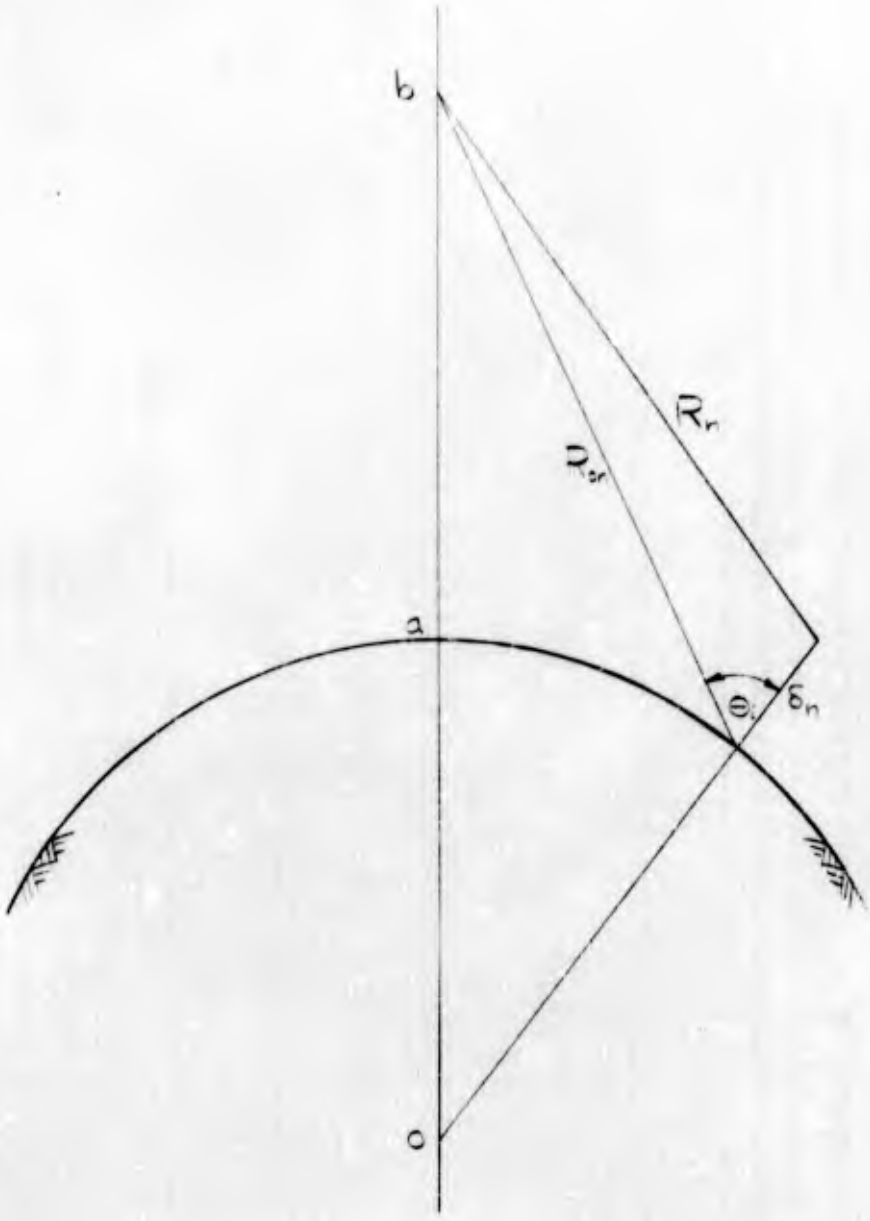

Figure 2.1

Neglecting the δ_n^2 term (as it is assumed $\delta_n^2 \ll R_{on}^2$),

$$R_n \approx R_{on}\left[1 - \frac{2\delta_n \cos\theta_i}{R_{on}}\right]^{\frac{1}{2}} . \qquad (2.5)$$

Expanding the square root by the binomial expansion and again neglecting all terms containing δ_n to powers greater than unity,

$$R_n \approx R_{on} - \delta_n \cos\theta_i . \qquad (2.6)$$

Substituting the above expression into the expressions for the field strength reradiated back to the source,

$$F \approx \sum_n \frac{e^{-j2k(R_{on} - \delta_n \cos\theta_i)}}{(R_{on} - \delta_n \cos\theta_i)^2} \Delta A_n$$

$$\approx \sum_n \frac{e^{-j2k(R_{on} - \delta_n \cos\theta_i)}}{R_{on}^2} \Delta A_n . \qquad (2.7)$$

It is assumed that variations due to the factor $\delta_n \cos\theta_i$ in the inverse square term are insignificant compared to the variations associated with the phase term.

Rewriting Equation (2.7) and expanding part of the exponential into the cis form,

$$F \approx \sum_n \frac{e^{-j2kR_{on}}}{R_{on}^2} e^{j2k\delta_n \cos\theta_i} \Delta A_n$$

$$\approx \sum_n \frac{e^{-j2kR_{on}}}{R_{on}^2} [\cos(2k\delta_n \cos\theta_i)$$

$$+ j\sin(2k\delta_n \cos\theta_i)] \qquad (2.8)$$

Defining a new quantity as

$$\Delta\varphi_n = 2k\delta_n \cos\theta_i \,, \tag{2.9}$$

$$F \approx \sum_n \frac{e^{-j2kR_{on}}}{R_{on}^2} (\cos\Delta\varphi_n + j\sin\Delta\varphi_n)\,\Delta A_n \,. \tag{2.10}$$

Assuming a normal distribution for δ_n results in the sine term having a zero mean value and the cosine term having a finite mean value. Denoting the mean value of the cosine term by $\overline{\cos\Delta\varphi_n}$, Equation (2.10) may be written

$$F \approx \sum_n \frac{e^{-j2kR_{on}}}{R_{on}^2}\,\overline{\cos\Delta\varphi_n}\;\Delta A_n + \sum_n \frac{e^{-j2kR_{on}}}{R_{on}^2}(\cos\Delta\varphi_n - \overline{\cos\Delta\varphi_n} + j\sin\Delta\varphi_n)\,\Delta A_n \,. \tag{2.11}$$

The normal distribution for the deviation δ_n from the mean surface is

$$p(\delta_n) = \frac{e^{-\frac{\delta_n^2}{2\sigma^2}}}{\sigma\sqrt{2\pi}} \tag{2.12}$$

where σ is the standard deviation of the scatterers from the mean surface. The mean value of the cosine may be computed by

$$\overline{\cos\Delta\varphi_n} = \overline{\cos(2k\delta_n\cos\theta_i)} = \int_{-\infty}^{\infty} \frac{e^{-\frac{\delta_n^2}{2\sigma^2}}}{\sigma\sqrt{2\pi}} \cos(2k\delta_n\cos\theta_i)\,d\delta_n \,. \tag{2.13}$$

From the integral tables,

$$\overline{\cos\Delta\varphi_n} = e^{-2(k\sigma\cos\theta_i)^2} \,. \tag{2.14}$$

Note that $\cos^2\theta_i$ appears as a multiplying factor in the mean value of the phase, where θ_i is the angle of incidence made by a range vector from the source to the point in question. Since the mean value of the phase, $\overline{\cos \Delta\varphi_n}$, varies slowly as a function of θ_i, it is essentially the same for any set of area elements near the point of zero angle of incidence. This is shown graphically in Figure 2.2. If the field strength is to be resolved into specular and non-specular components, the specular component should not vary with θ_i. For this reason $\cos\theta_i$ is set equal to unity and a new quantity, x, is defined as

$$x = \lim_{\theta_i \to 0} \cos\Delta\varphi_n = \lim_{\theta_i \to 0} e^{-2(k\sigma\cos\theta_i)^2} = e^{-2k^2\sigma^2} \qquad (2.15)$$

Thus the field strength becomes

$$F \approx \sum_n \frac{x\, e^{-j2kR_{on}}}{R_{on}^2} + \sum_n \frac{e^{-j2kR_{on}}}{R_{on}^2}\left|\cos\Delta\varphi_n - x + j\sin\Delta\varphi_n\right|$$

which may be written as

$$F \approx x F_{spec} + F_{rand} \qquad (2.16)$$

The physical significance of Equation (2.16) is that the field strength returned from a rough surface is made up of a fading and non-fading component. This combination of specular and random components is present all the time; however, Figure 2.2 indicates that it may be difficult to find surfaces which will return measurable amounts of both components.

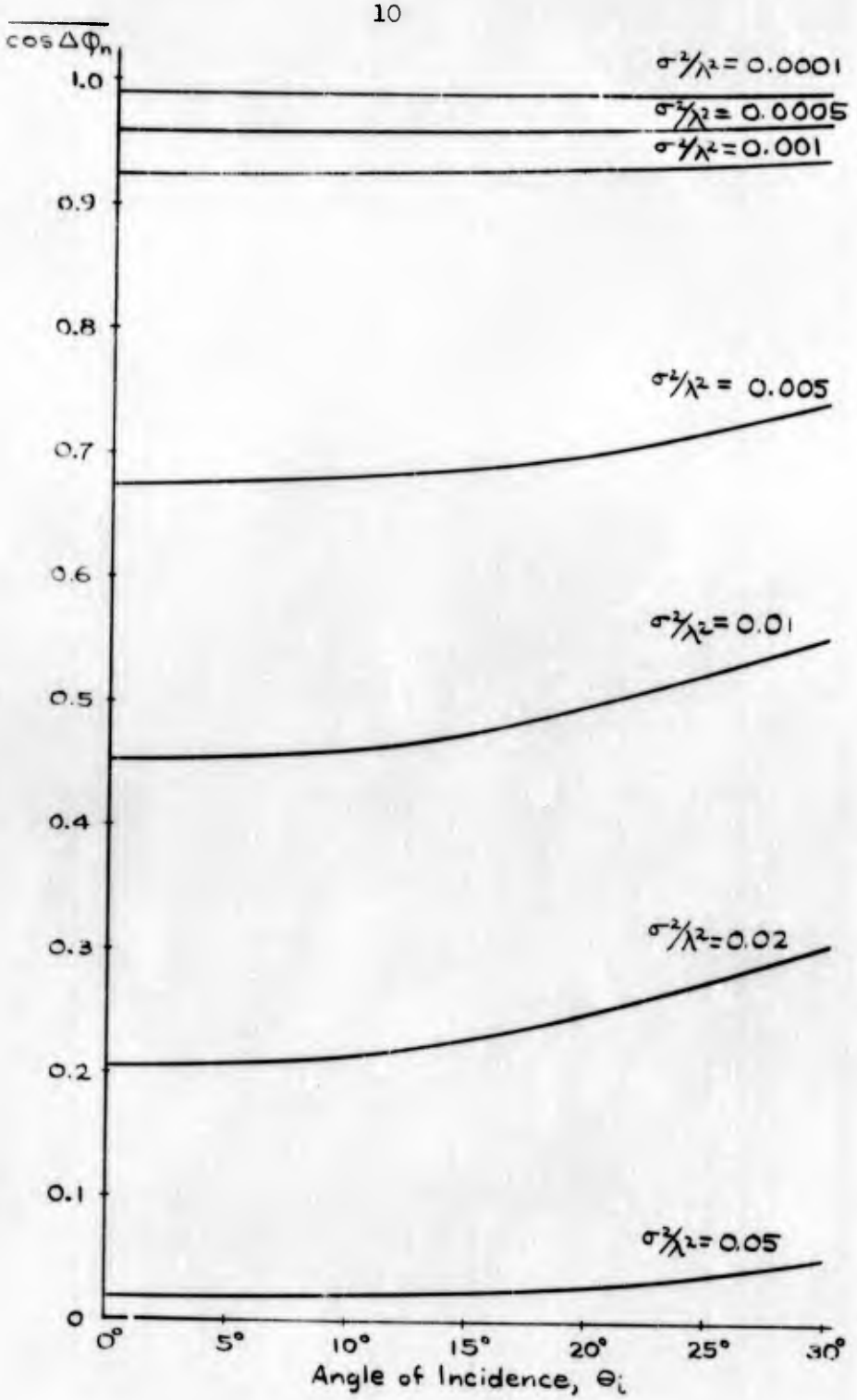
cos Δφn
1.0
0.9
0.8
0.7
0.6
0.5
0.4
0.3
0.2
0.1
0
σ²/λ² = 0.0001
σ²/λ² = 0.0005
σ²/λ² = 0.001
σ²/λ² = 0.005
σ²/λ² = 0.01
σ²/λ² = 0.02
σ²/λ² = 0.05
0°
5°
10°
15°
20°
25°
30°
Angle of Incidence, θi

Figure 2.2

CHAPTER III

SPECULAR REFLECTIONS FROM A SPHERE

In the preceding Chapter the field strength reflected from an arbitrary rough surface was separated into two components; a specular and a scatter component. This Chapter contains the derivation of the analytic form for the specular power reflected from a smooth sphere.

V. A. Fock has derived the expressions for the case of the reflection of an arbitrary wave from an arbitrary surface.[9] Only the applicable results of Fock's development will be utilized here. Fock's boundary conditions are given in Appendix A for the interested reader.

The geometry of the problem is shown in Figure 3.1. The origin of the spherical coordinate system r_a, θ_a, ϕ_a is at the center of the sphere of radius a. Let the source of energy be a small current element, located in the point $r_a = b > a$, $\theta_a = 0^\circ$, with a wavelength $\lambda \ll a$, and oriented so the axis of the current element is perpendicular to a line drawn from the center of the sphere through the mid-point of the current element.

For the moment, a new coordinate system is required; it will soon be discarded. The new system is also spherical and

---

[9] Fock, V. A., op. cit.

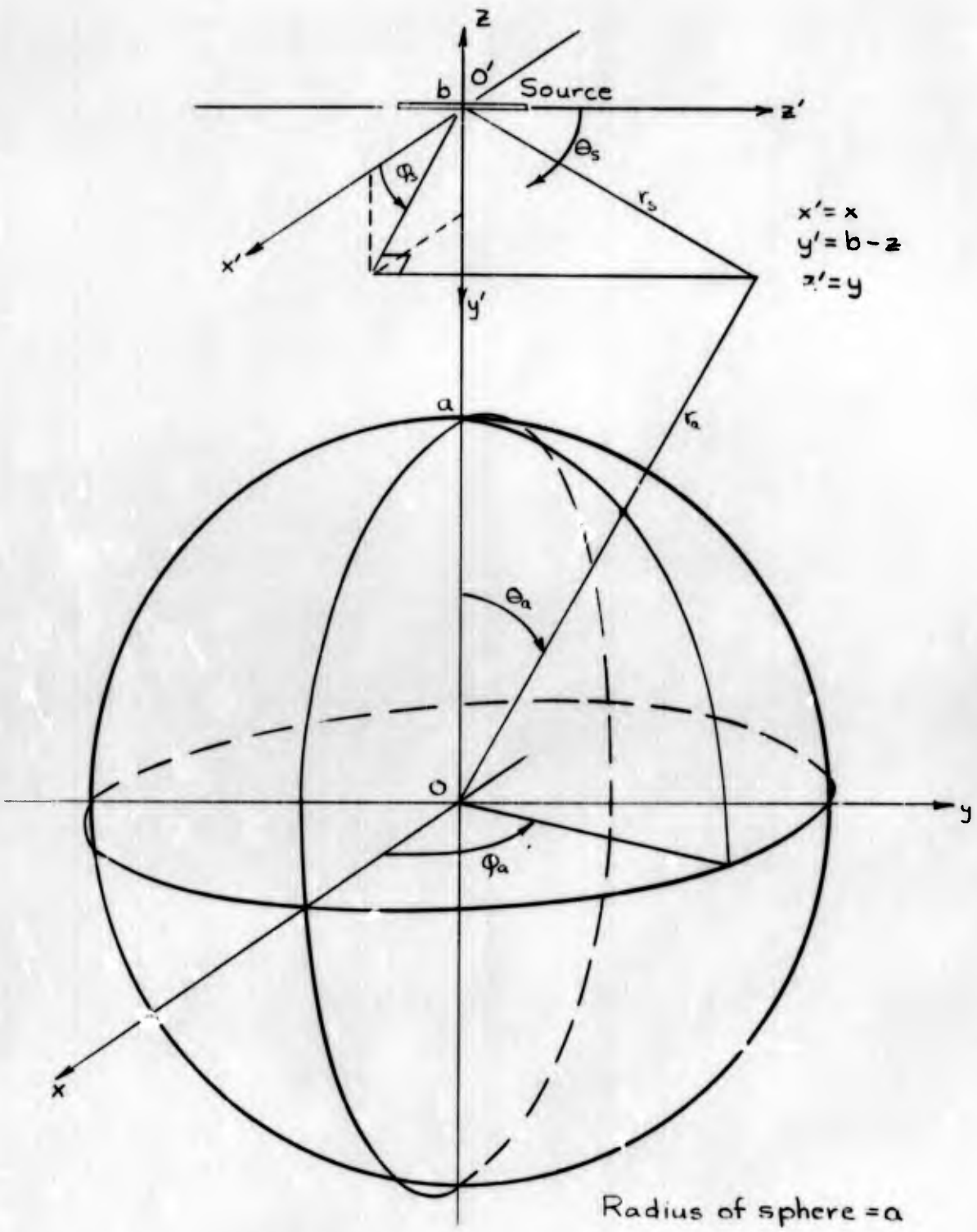
z
O'
b
Source
z'
θ_s
φ_s
r_s
x'
x' = x
y' = b - z
z' = y
y'
a
r_a
θ_a
O
y
φ_a
x
Radius of sphere = a

Figure 3.1

denoted by r_s, θ_s, ϕ_s with its origin at the center of the small current element. In terms of the new coordinate system the electric field of the linear current element is

$$\underline{E} = j\frac{\omega\mu I_o \ell}{4\pi r_s} \sin\theta_s e^{-jkr_s} \underline{u}_{\theta_s} , \tag{3.1}$$

where $\underline{E}$ is radiated field at distances such that $r_s^2 >> r_s$,

r_s is distance from the source,

ω is angular frequency,

I_o is current,

ℓ is length of the element,

μ is magnetic permeability,

$\underline{u}_{\theta_s}$ is unit vector in the θ_s direction,

j is $\sqrt{-1}$

As it is more convenient to utilize Fock's work in terms of the coordinate system with the origin at the center of the sphere, the expression for $\underline{E}$ is translated into that system.

From the geometry of Figure 3.1,

$$r_s^2 = r_a^2 + b^2 - 2r_a b\cos\theta_a , \tag{3.2}$$

$$\sin\theta_s = \left[1 - \frac{z'^2}{r_s^2}\right]^{1/2} = \left[\frac{r_a^2 + b^2 - 2r_a b\cos\theta_a - y^2}{r_a^2 + b^2 - 2r_a b\cos\theta_a}\right]^{1/2} , \tag{3.3}$$

$$\underline{u}_{\theta_s} = \left[\underline{i}\, xy - \underline{j}(-2r_a b\cos\theta_a - y^2 + r_a^2 + b^2) - \underline{k}\, y(b-z)\right]$$

$$\cdot \left[(r_a^2 + b^2 - 2r_a b\cos\theta_a - y^2)(r_a^2 + b^2 - 2r_a b\cos\theta_a)\right]^{-1/2} . \tag{3.4}$$

Substituting these expressions into Equation (3.1),

$$\underline{E} = \frac{j\omega\mu I_o \ell \, e^{-jk(r_a^2+b^2-2r_a b\cos\theta_a)^{1/2}}}{4\pi\left[r_a^2+b^2-2r_a b\cos\theta_a\right]^{3/2}}\left[\underline{i}\,x y - \underline{j}(r_a^2+b^2-2r_a b\cos\theta_a - y^2) + \underline{k}\,y(z-b)\right] . \quad (3.5)$$

The complex scalar magnitude of $\underline{E}$ is

$$E = \frac{j\omega\mu I_o \ell \,(r_a^2+b^2-2r_a b\cos\theta_a - y^2)^{1/2}}{4\pi(r_a^2+b^2-2r_a b\cos\theta_a)} e^{-jk(r_a^2+b^2-2r_a b\cos\theta_a)^{1/2}} \quad (3.6)$$

Denoting the incident field at the surface of the sphere by E_i, then at $r_a = a$,

$$E_i = \frac{j\omega\mu I_o \ell (a^2+b^2-2ab\cos\theta_a - y^2)^{1/2}}{4\pi(a^2+b^2-2ab\cos\theta_a)} e^{-jk(a^2+b^2-2ab\cos\theta_a)^{1/2}} . \quad (3.7)$$

By Fock's development, the magnitude of the field reflected to a probe a distance R' from the surface of the sphere is

$$E_p = E_{io}\, e^{-jkR} \sqrt{\frac{D(0)}{D(R')}}\; e^{-jkR'} , \quad (3.8)$$

where E_p is the reflected field received by the probe,

E_{io} is the reflected field at the surface of the sphere,

R is the range from the source to the point of incidence,

R' is the range from the point of incidence to the probe,

D(0)/D(R') is Fock's dispersion factor (specialized to the sphere) for the reflected wave with

$$R^2 D(R') = \left[(R+R')\cos\theta_i + \frac{2RR'}{a}\right]\left[(R+R') + \frac{2RR'}{a}\cos\theta_i\right] \quad (3.9)$$

θ_i is the angle of incidence.

The geometry of this situation is shown in Figure 3.2.

The vector $\underline{E}_{io}$ will be a very complicated expression as it contains $\underline{E}_i$ which has already been complicated by a translation of coordinate systems and the polarization of $\underline{E}_i$ will be some combination of vertical and horizontal polarization. The exact form of $\underline{E}_{io}$ will be of no use in the final result; hence, only E_{io} will be determined.

The distance, R', from the point of incidence to the probe is given by

$$R' = -a\cos\theta_i \pm (a^2\cos^2\theta_i - a^2 + r_a^2)^{1/2} . \tag{3.10}$$

As $R' > 0$,

$$R' = (-a^2\sin^2\theta_i + r_a^2)^{1/2} - a\cos\theta_i . \tag{3.11}$$

Now

$$R^2 D(0) = R^2\cos\theta_i \tag{3.12}$$

or

$$D(0) = \cos\theta_i . \tag{3.13}$$

Thus

$$\sqrt{\frac{D(0)}{D(R')}} = \left\{ \frac{R^2\cos\theta_i}{\left[(R'+R)\cos\theta_i + \frac{2R'R}{a}\right]\left[(R'+R) + \frac{2R'R\cos\theta_i}{a(R'+R)}\right]} \right\}^{1/2} \tag{3.14}$$

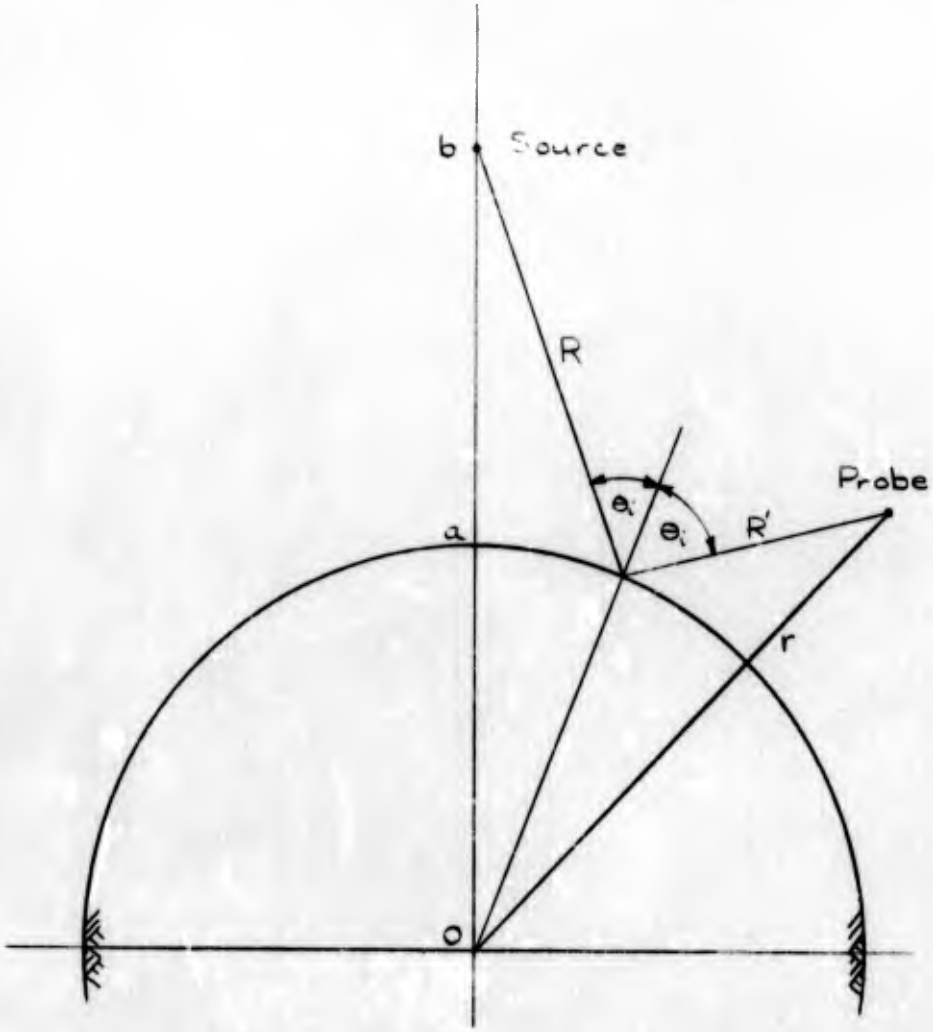

Figure 3.2

Then

$$E_p = \frac{E_{io}\, R\, e^{-jk(R+R')}}{R+R'} \left\{ \frac{\cos\theta_i}{\left[\cos\theta_i + \frac{2RR'}{a(R+R')}\right]\left[1 + \frac{2RR'}{a(R+R')}\cos\theta_i\right]} \right\}^{1/2} \tag{3.15}$$

The power density, S_p, at the probe is

$$S_p = \frac{1}{2} \mathrm{Re} \frac{\underline{E}_p \cdot \underline{E}_p^*}{\eta} \tag{3.16}$$

where η is the intrinsic impedance of the medium and $\underline{E}_p^*$ is the complex conjugate of $\underline{E}_p$. Hence

$$S_p = \frac{|E_{io}|^2 R^2}{2\eta (R+R')^2} \left\{ \frac{\cos\theta_i}{\left[\cos\theta_i + \frac{2RR'}{a(R+R')}\right]\left[1 + \frac{2RR'}{a(R+R')}\cos\theta_i\right]} \right\} \tag{3.17}$$

If the probe and the source are one and the same, the above expression may be simplified as

$$R = R' = b - a = h \,, \tag{3.18}$$

and

$$\cos\theta_i = \cos 0^\circ = 1 \,. \tag{3.19}$$

The remaining quantity needed is E_{io}. The theory of reflection as developed by Fock contains the Fresnel reflection coefficients which are depenedent on the angle of incidence and these also become simpler when $\theta_i = 0^\circ$. For this condition

$$|E_{io}| = |K||E_i| \,, \tag{3.20}$$

where K is the appropriate reflection coefficient and E_i is the incident wave at the surface of the sphere. Thus

$$|E_i| = \frac{\omega\mu I_o l}{4\pi(b-a)} \tag{3.21}$$

The power density reflected from the sphere to the point of the source is then

$$S_p = \frac{\mu^2 \omega^2 I_o^2 \ell^2 |K|^2 a^2}{2\eta (4\pi)^2 (2h^2)(a+h)^2} \quad . \tag{3.22}$$

This result may be put into a more useful form as follows. The transmitted power density, S_T, is

$$S_T = \frac{\mu^2 \omega^2 I_o^2 \ell^2}{2\eta (4\pi)^2 R^2} \sin^2 \theta_s = \frac{P_T G}{4\pi R^2} \sin^2 \theta_s \, , \tag{3.23}$$

from which

$$P_T G = \frac{\mu^2 \omega^2 I_o^2 \ell^2}{2\eta (4\pi)} \tag{3.24}$$

where G is the maximum antenna gain and P_T is the transmitted power. Thus the total received power, P_r, is

$$P_r = S_p A_{eff} = \frac{P_T G^2 \lambda^2 |K|^2}{(4\pi)^2 (2h)^2 (1 + h/a)^2} \tag{3.25}$$

where

$$A_{eff} = \frac{G \lambda^2}{4\pi} \quad . \tag{3.26}$$

CHAPTER IV

THE EQUATION OF SCATTER POWER RETURN

R. K. Moore and C. S. Williams have developed an expression for the scatter power returned from an arbitrary scattering surface.[10] The result is restricted to surfaces which have mean radii of curvature that are many wavelengths long.

In terms of the geometry of Figure 4.1, Moore and Williams' result is

$$\overline{P_r(d)} = \frac{\lambda^2}{(4\pi)^3} \int_A \frac{P_T(d - \frac{2R}{c})\, G^2(\theta_s, \varphi)\, \sigma_o(\theta_i, \varphi)\, dA}{R^4} \qquad (4.1)$$

where

$\overline{P_r(d)}$ is the average received pulse of an ensemble of received pulses,

$P_T(d - 2R/c)$ is the transmitted power,

$G(\theta_s, \varphi)$ is the antenna gain,

$\sigma_o(\theta_s, \varphi)$ is the mean scattering cross-section per unit area,

R is the radar range to an area element,

A is the irradiated area,

φ is the azimuth angle,

θ_s is the antenna angle,

θ_i is the angle of incidence.

---

[10] Moore and Williams, op. cit.

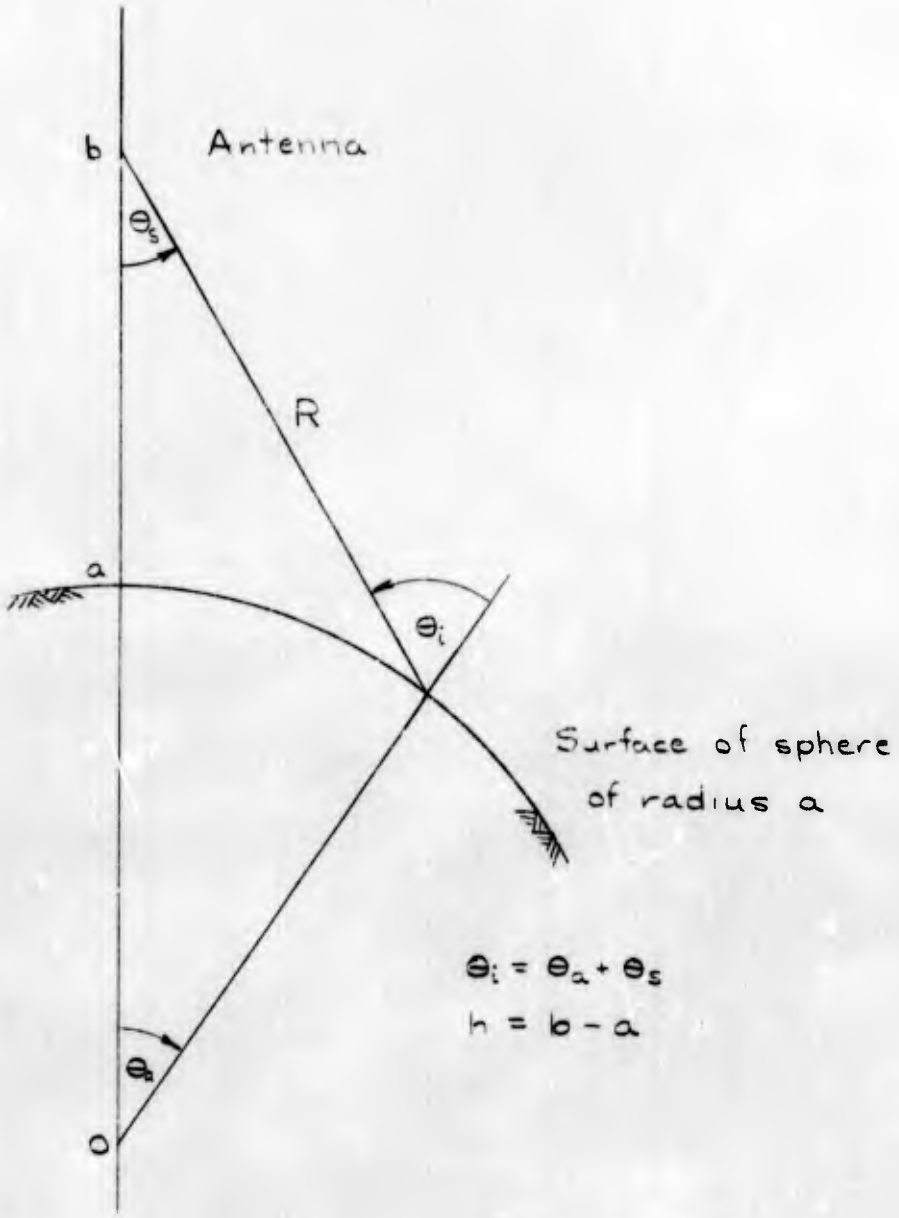
b
Antenna
θ_s
R
a
θ_i
Surface of sphere
of radius a
$\theta_i = \theta_a + \theta_s$
$h = b - a$
θ_a
o

Figure 4.1

The antenna is oriented such that

$$G(0°,\varphi) = G_{max} \cdot \tag{4.2}$$

The area element of the sphere of radius a is

$$dA = a^2 \sin\theta_a \, d\theta_a \, d\varphi \ . \tag{4.3}$$

At this point it is worthwhile to note that the actual area element is used in the above integral and not the effective area element as viewed from the antenna. In all the previous work on scattering done at the University of New Mexico, the multiplying factor, $\cos\theta_i$, for converting the actual area element to an effective area element, has been included in $\sigma_o(\theta_i,\varphi)$; it will be left in $\sigma_o(\theta_i,\varphi)$ throughout the remainder of this paper.

From Figure 4.1 and the cosine law,

$$R^2 = a^2 + b^2 - 2ab\cos\theta_a \ . \tag{4.4}$$

Taking the differential,

$$R\,dR = ab\sin\theta_a \, d\theta_a \ , \tag{4.5}$$

from which

$$dA = \frac{a}{b} R\,dR\,d\varphi \ . \tag{4.6}$$

Thus the power return integral becomes

$$P_r(d) = \frac{\lambda^2 a}{(4\pi)^3 b} \int_0^{2\pi} \int_h^{\frac{cd}{2}} \frac{P_T(d-\frac{2R}{c}) G^2(\theta_s,\varphi) \sigma_o(\theta_i,\varphi) dR\,d\varphi}{R^3}$$

$$= \frac{\lambda^2 a}{2(4\pi)^2 b} \int_h^{\frac{cd}{2}} \frac{P_T(d-\frac{2R}{c}) G^2(\theta_s) \sigma_o(\theta_i) dR}{R^3} \tag{4.7}$$

assuming no variation with φ in $G_1(\theta_s,\varphi)$ and $\sigma_o(\theta_i,\varphi)$.

This result may be put into a different form by defining a radar delay time, T.

The antenna is located at a distance h above the scattering surface as shown in Figure 4.2. The elapsed time required for the altitude signal to return to the antenna after transmission is $d = 2h/c$. Likewise, the elapsed time required for the range signal to return to the antenna after tramsmission is

$$d' = \frac{2R}{c} \quad , \quad d' > d \; . \tag{4.8}$$

Let $T = d' - d$ be the delay time between the altitude signal and

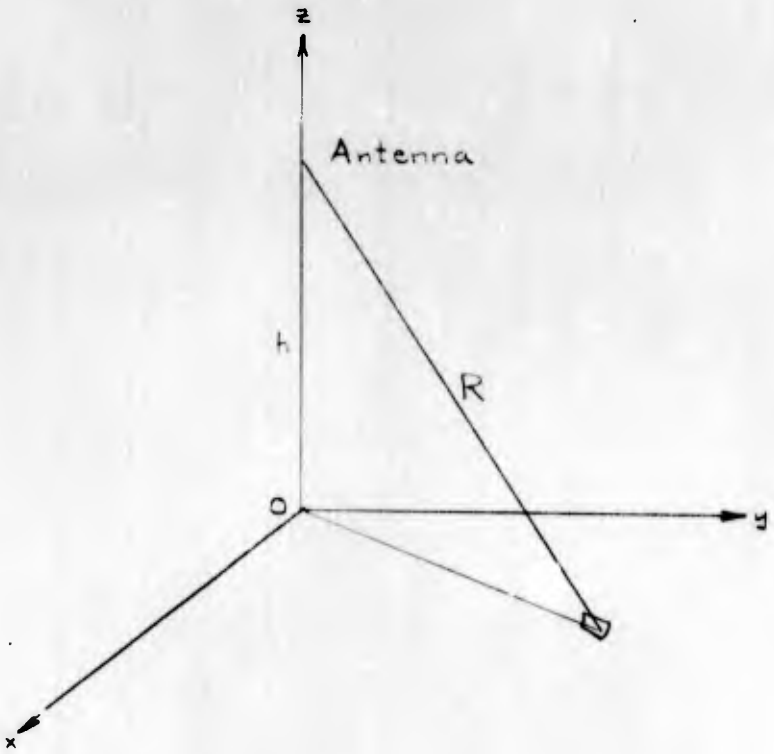

Figure 4.2

the range signal. Then

$$T = \frac{2}{c}(R-h), \tag{4.9}$$

or

$$R = \frac{cT}{2} + h \tag{4.10}$$

from which

$$dR = \frac{c}{2}dT \ . \tag{4.11}$$

Now the power return integral may be written as

$$\overline{P_r(d)} = \frac{c\lambda^2 a}{4(4\pi)^2 b}\int_0^{d-\frac{2h}{c}} \frac{P_T(d-T-\frac{2h}{c})\,G^2(\theta_s)\,\sigma_0(\theta_i)\,dT}{(h+\frac{cT}{2})^3} \tag{4.12}$$

Note that θ_s and θ_i are both functions of R, hence they are both functions of T.

Since

$$\overline{P_r(d)} = 0 \quad , \quad d \le \frac{2h}{c} \ , \tag{4.13}$$

$$\overline{P_r(d)} \neq 0 \quad , \quad \frac{2h}{c} < d \ , \tag{4.14}$$

the time argument of the integral may be changed to a modified delay time such that

$$\overline{P_r(d+\tfrac{2h}{c})} = 0 \ , \ d \le 0 \ , \tag{4.15}$$

$$\overline{P_r(d+\tfrac{2h}{c})} \neq 0, \quad 0 < d \ . \tag{4.16}$$

Hence

$$\overline{P_r(d+\tfrac{2h}{c})} = \frac{c\lambda^2 a}{4(4\pi)^2 b}\int_0^{d} \frac{P_T(d-T)\,G^2(\theta_s)\,\sigma_0(\theta_i)}{(h+\frac{cT}{2})^3}\,dT \tag{4.17}$$

CHAPTER V

TOTAL POWER RETURN

1. Total Power Return from a Rough Spherical Surface

In the previous chapters, expressions for specular power return from a smooth sphere and scatter power return from a rough sphere were developed. As it is desired to resolve the power return from near (and including) vertical incidence into two components, the two expressions for power return must be combined in some manner.

It has been shown that the field strength may be separated into two components; a specular component reduced by $x \leq 1$, and a scatter component. If the specular field is reduced by x, then the specular power must be reduced by x^2; hence, the scatter power is reduced by $(1-x^2)$. Thus, the total power return may be written as

$$\overline{P_r\left(d+\frac{2h}{c}\right)} = \frac{P_T(d)\,G^2(0^\circ)\,\lambda^2 a^2 x^2 |K|^2}{(4\pi)^2 (2h)^2 b^2} + \frac{c\lambda^2 a_1 \beta (1-x^2)}{4(4\pi)^2 b}\int_0^d \frac{P_T(d-T)\,G^2(\theta_2)\,\sigma_0(\theta_1)\,dT}{\left(h+\frac{cT}{2}\right)^3} \qquad (5.1)$$

Here the factor β has been included to account for absorption and depolarization in an imperfect terrain.

This equation for the power return has been developed for a spherical wave front irradiating a rough spherical surface. However, there is one other result of immediate interest which is easily derived from this equation; that of a spherical wave

irradiating a rough plane surface.

Note that both terms in the equation contain the factor a/b; the ratio of the mean radius of the sphere to the distance of the source from the center of the sphere. Recalling that b=a+h, where h is the height of the source above the mean surface of the sphere,

$$\frac{a}{b} = \frac{1}{1+h/a} \tag{5.2}$$

Consideration of the case $h/a \ll 1$ leads to the equations for a spherical wave irradiating a rough plane.

2. Total Power Return from a Rough Plane

If $h/a \ll 1$, then $a/b \approx 1$. An application of the law of sines to the geometry of Figure 4.1 leads to

$$\frac{\sin\theta_s}{a} = \frac{\sin\theta_i}{a+h} \tag{5.3}$$

or

$$\sin\theta_s = \frac{\sin\theta_i}{1+h/a} \approx \sin\theta_i . \tag{5.4}$$

Hence $G(\theta_s) \approx G(\theta_i)$. The equation of power return is then

$$\overline{P_r(d+\tfrac{2h}{c})} = \frac{P_T(d)\, G^2(0^\circ)\, \lambda^2\, x^2 |K|^2}{(4\pi)^2 (2h)^2}$$

$$+ \frac{c\lambda^2 \beta (1-x^2)}{4(4\pi)^2} \int_0^d \frac{P_T(d-T)\, G^2(\theta_i)\, \sigma_0(\theta_i)\, dT}{(h+cT/2)^3} \tag{5.5}$$

This equation has been derived by Moore for the case of a spherical wave front scattered by a rough plane.[11]

The maximum altitude at which this equation is valid depends upon the error that can be tolerated resulting from the approximations

$$\frac{a}{b} \approx 1 \tag{5.6}$$

and

$$\theta_s \approx \theta_i \tag{5.7}$$

For example, by considering the factor a/b at an altitude of 400 miles above earth, the specular power is reduced by

$$20 \log\left(1 + \frac{400}{4000}\right) db = 0.82\ db \tag{5.8}$$

and the scatter power is reduced by 0.41 db. Since the approximation $\theta_s \approx \theta_i$ affects only the antenna gain, it is more difficult to estimate the error in scatter power resulting from this approximation. However, θ_i increases more rapidly than θ_s and this will tend to make the antenna pattern appear narrower than it actually is. This in turn will cause the computed scatter power to be less in magnitude along the trailing edge of the return pulse. A graph of θ_s versus θ_i with h/a as a parameter is shown in Figure 5.1.

---

[11] Moore, R. K., op. cit., Tech. Report EE-6.

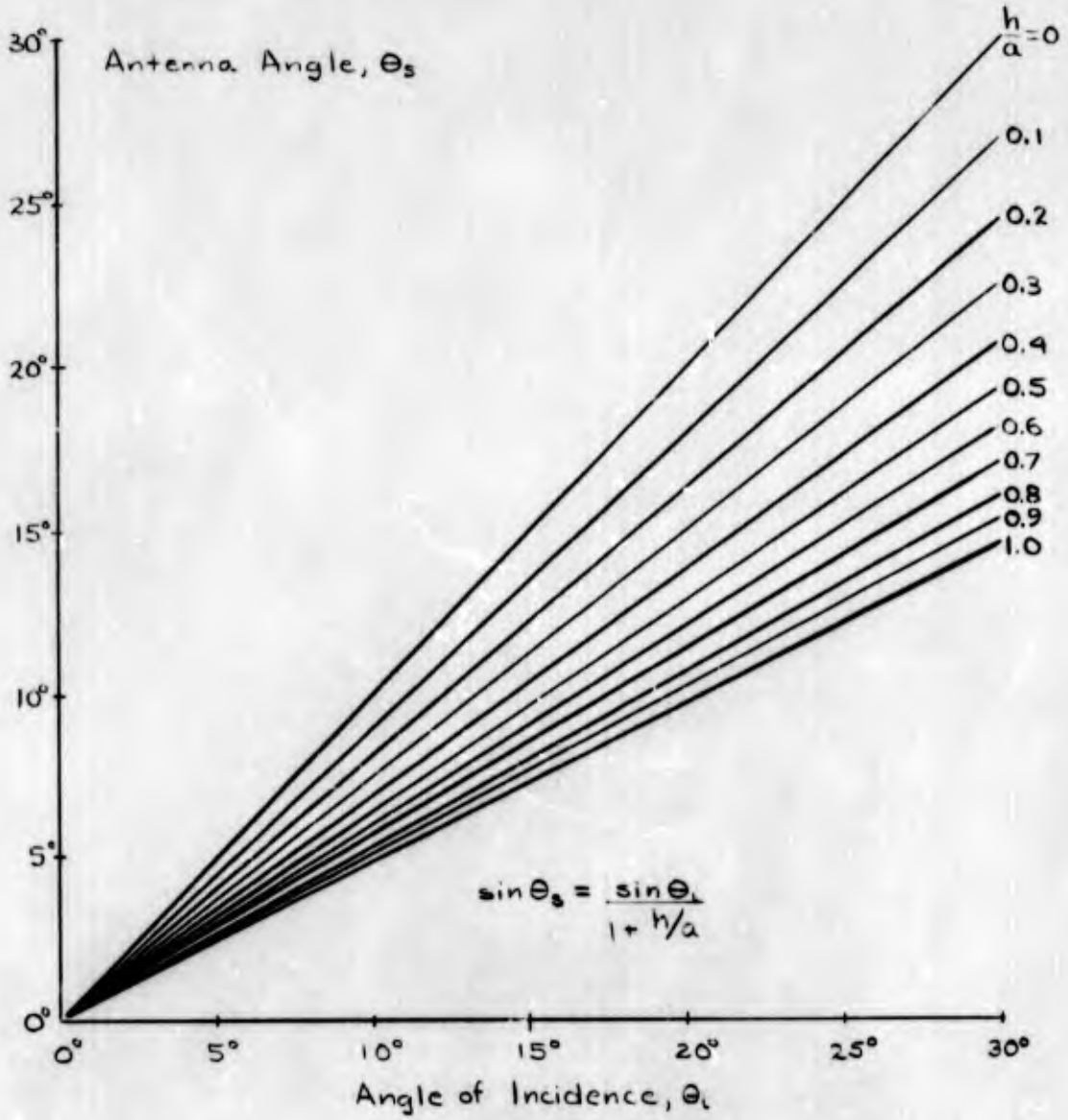
Antenna Angle, θ_s
30°
25°
20°
15°
10°
5°
0°
$\frac{h}{a}=0$
0.1
0.2
0.3
0.4
0.5
0.6
0.7
0.8
0.9
1.0
$\sin\theta_s = \frac{\sin\theta_i}{1+h/a}$
0°
5°
10°
15°
20°
25°
30°
Angle of Incidence, θ_i

Figure 3.1

CHAPTER VI

A THEORETICAL MODEL FOR THE SCATTERING CROSS SECTION, $\sigma_o(\theta_i)$

1. An Exact Integral Form

In the preceding Chapters it has been shown that

(i) the power return from a rough surface may be separated into two components; a specular component and a scatter component.

(ii) the specular power return from a rough surface is equal to the return from a smooth surface reduced by a multiplying factor which depends upon surface roughness.

(iii) the scatter power return is obtained from a convolution integral containing a scattering cross-section, $\sigma_c(\theta_i)$, which is an unknown analytic quantity at this point.

An analytic form for the scattering cross-section is desirable for predicting the scatter power returned from a rough target.

The only feasible way to approach this problem is in terms of the statistics of a rough target. It has been shown that the field strength returned from a rough target may be separated into two components with the assumption that the Gaussian or normal probability density function may be used to describe the scatters. A similar procedure will be followed in developing a theoretical scattering cross-section for the

rough target. Davies [12] and Moore[13] have attempted the same problem and the following work is similar to theirs; however, a few departures are made from the procedures followed by them.

The electric field received at a point in space due to the currents which flow on a perfectly conducting surface as a result of irradiation by an elevated isotropic source is given by Huygen's - Kirchhoff integral as

$$E = \int_A \sqrt{\frac{P_T \eta}{4\pi R^2}} \frac{e^{-j2kR}}{\lambda R} \cos\theta_i \, dA \quad , \qquad (6.1)$$

where

$\sqrt{\frac{P_T \eta}{4\pi R^2}}$ is the intensity of radiation on an area element,

R is the range to an area element,

η is the impedance of the medium containing the source,

λ is wavelength,

θ_i is the angle of incidence between the incident Poynting vector and the normal to the area element.

The integral as written above implies that the source and receiver are located in the same point. The power received at that point is given by

$$P_r = \frac{1}{2} \mathrm{Re} \frac{EE^*}{\eta} A_r \quad , \qquad (6.2)$$

---

[12] Davies, H., op. cit.

[13] Moore, R. K., op. cit., Tech Report EE-6

where E^* is the conjugate of E and A_r is the effective area of the isotropic receiving antenna.

The received power may be written in terms of the integral as

$$P_r = \frac{A_r}{2\eta} \mathcal{R}e \int_A \sqrt{\frac{P_T \eta}{4\pi}} \frac{e^{-j2kR}}{\lambda R^2} \cos\theta_i \, dA \int_{A'} \sqrt{\frac{P_T \eta}{4\pi}} \frac{e^{j2kR'}}{\lambda R'^2}$$

$$\cdot \cos\theta_i' \, dA' \tag{6.3}$$

where the primed quantities refer to a different point than the unprimed quantities since the integrals must be taken separately. This expression may be written in the form

$$P_r = \mathcal{R}e \frac{A_r}{8\pi\lambda^2} \int_A \int_{A'} \frac{P_T \, e^{-j2k(R-R')}}{R^2 R'^2} \cos\theta_i \cos\theta_i' \, dA \, dA' . \tag{6.4}$$

It is now apparent that R and R' are statistically related in some manner in terms of the target roughness parameters.

In Chapter II it was found that

$$R = R_o - \delta \cos\theta_i \tag{6.5}$$

and hence

$$R' = R_o' - \delta' \cos\theta_i' \tag{6.6}$$

It is necessary to define the coordinates and some new variables for the integration; these are shown in Figure 6.1. The area element dA is located in point A' and dA' is located in point B'. Point D is used only for the purpose of defining

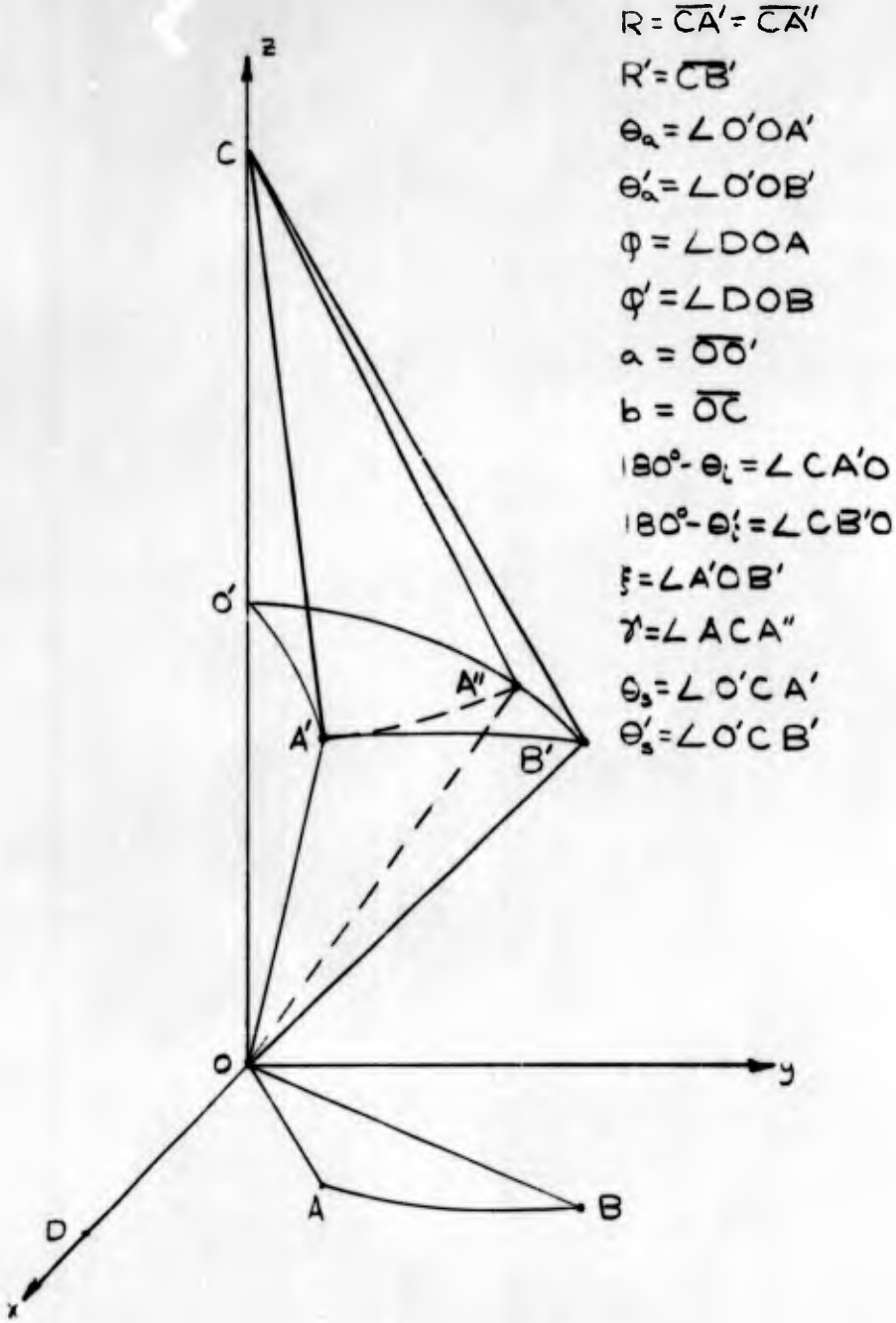
z
C
O'
A''
A'
B'
O
y
D
x
A
B
$R = \overline{CA'} = \overline{CA''}$
$R' = \overline{CB'}$
$\theta_a = \angle O'OA'$
$\theta_a' = \angle O'OB'$
$\varphi = \angle DOA$
$\varphi' = \angle DOB$
$a = \overline{OO'}$
$b = \overline{OC}$
$180° - \theta_i = \angle CA'O$
$180° - \theta_i' = \angle CB'O$
$\xi = \angle A'OB'$
$\gamma = \angle ACA''$
$\theta_s = \angle O'CA'$
$\theta_s' = \angle O'CB'$

Figure 6.1

the angles φ and φ'; the distance OD has no significance. The area O'A'B'O' is a portion of the spherical surface of radius a and the area OABO is the projection of O'A'B'O' on the xy-plane.

The primed quantities may be associated with the unprimed quantities by defining the new variables of integration s, ζ, and γ as

$$R_o' = R_o + s \,, \tag{6.7}$$

$$\varphi' = \varphi + \zeta \,, \tag{6.8}$$

$$\theta_a' = \theta_a + \gamma \,, \tag{6.9}$$

where s, ζ, and γ represent, respectively, the change in range, change in longitude, and change in co-latitude in going from A' to B'.

The area elements of integration are given by

$$dA = a^2 \sin\theta_a \, d\theta_a \, d\varphi \,, \tag{6.10}$$

$$dA' = a^2 \sin\theta_a' \, d\theta_a' \, d\varphi' \,. \tag{6.11}$$

From the geometry of Figure 6.1

$$R^2 = a^2 + b^2 - 2ab\cos\theta_a \,, \tag{6.12}$$

$$R'^2 = a^2 + b^2 - 2ab\cos\theta_a' \,. \tag{6.13}$$

Taking the differentials of these equations,

$$R\,dR = ab\sin\theta_a \, d\theta_a \,, \tag{6.14}$$

$$R'dR' = ab\sin\theta_a' \, d\theta_a' \,. \tag{6.15}$$

Hence, the area elements can be expressed as

$$dA = \frac{a}{b} R\,dR\,d\varphi \quad , \tag{6.16}$$

$$dA' = \frac{a}{b} R'\,dR'\,d\varphi' \quad . \tag{6.17}$$

As the integration requires that the primed quantities be integrated while the unprimed quantities are held constant,

$$dR' = d(R+s) = ds \quad , \tag{6.18}$$

$$d\varphi' = d(\varphi+\zeta) = d\zeta \quad . \tag{6.19}$$

Substituting these results into the expression for received power,

$$P_r = \frac{A_r a^2}{8\pi\lambda^2 b^2} \iiint_A \iiint_{A'} \frac{P_T e^{-j2k(s-\delta\cos\theta_i+\delta'\cos\theta_i')}}{RR'} \cos\theta_i \cos\theta_i'\, dR\,d\varphi\,ds\,d\zeta \, . \tag{6.20}$$

Additional information is required for the quantities δ and δ' before the integration can be carried out. It should be recalled that δ and δ' are actual physical deviations of the surface of the sphere from the mean spherical surface. The deviation δ has already been described by the normal probability density function

$$p(\delta) = \frac{e^{-\delta^2/2\sigma^2}}{\sigma\sqrt{2\pi}} \tag{6.21}$$

in the process of separating specular and scatter field components. If it is assumed that some correlation exists between δ and δ', and that these two variates are normally distributed, then it may be reasonable to assume that δ and δ' can be described by the normal bivariate probability

density function

$$p(\delta,\delta') = \frac{e^{-\frac{(\delta^2 + 2\rho\delta\delta' + \delta'^2)}{2\sigma^2(1-\rho^2)}}}{2\pi\sigma^2\sqrt{1-\rho^2}} \tag{6.22}$$

where ρ is the correlation between δ and δ'. With these assumptions, the mean or expected value of

$$f(\delta,\delta') = e^{-j2k(\delta'\cos\theta_i' - \delta\cos\theta_i)} \tag{6.23}$$

may be computed from the relationship

$$\overline{f(\delta,\delta')} = E[f(\delta,\delta')] = \int_{-\infty}^{\infty}\int_{-\infty}^{\infty} f(\delta,\delta')\, p(\delta,\delta')\, d\delta\, d\delta' \; ; \tag{6.24}$$

$$\overline{f(\delta,\delta')} = \int_{-\infty}^{\infty}\int_{-\infty}^{\infty} \frac{e^{-j2k(\delta'\cos\theta_i' - \delta\cos\theta_i) - \frac{(\delta^2 + 2\rho\delta\delta' + \delta'^2)}{2\sigma^2(1-\rho^2)}}}{2\pi\sigma^2\sqrt{1-\rho^2}}\, d\delta\, d\delta' . \tag{6.25}$$

Integrating on δ,

$$\int_{-\infty}^{\infty} e^{-j2k\delta\cos\theta_i - \frac{\delta^2}{2\sigma^2(1-\rho^2)} - \frac{2\rho\delta\delta'}{2\sigma^2(1-\rho^2)}}\, d\delta$$

$$= \sqrt{2\pi}\,\sigma\sqrt{1-\rho^2}\; e^{\frac{\rho^2\delta'^2}{2\sigma^2(1-\rho^2)} - j2k\rho\delta'\cos\theta_i - 2k^2\sigma^2(1-\rho^2)\cos^2\theta_i} \tag{6.26}$$

Integrating on δ',

$$\int_{-\infty}^{\infty} e^{-j2k\delta'\cos\theta_i' - \frac{\delta'^2}{2\sigma^2(1-\rho^2)} + \frac{\rho^2\delta'^2}{2\sigma^2(1-\rho^2)} - j2k\rho\delta'\cos\theta_i}\, d\delta'$$

$$= \sqrt{2\pi}\,\sigma\; e^{-2k^2\sigma^2[(\cos\theta_i' + \rho\cos\theta_i]^2} . \tag{6.27}$$

Combining these results,

$$\overline{f(\delta,\delta')} = e^{-2k^2\sigma^2(\cos^2\theta_i - 2\rho\cos\theta_i\cos\theta_i' + \cos^2\theta_i')} \tag{6.28}$$

In the process of describing $f(\delta,\delta')$ by the mean value, $\overline{f(\delta,\delta')}$, the correlation coefficient, ρ, has appeared in the final result and now requires a description.

Determining the proper correlation function for a statistical process seems to be a problem of major difficulty. The correlation function

$$\Gamma(r) = \rho(r)\Gamma_{max} \tag{6.29}$$

for a statistical process, $\delta(r)$, is defined as

$$\Gamma(r) = \lim_{r\to\infty} \frac{1}{2r}\int_{-r}^{r} \delta(\tau)\,\delta(r+\tau)\,d\tau \ . \tag{6.30}$$

In most cases, $\delta(r)$ is not a known analytic function; this represents the first problem in evaluating $\Gamma(r)$. However, in many cases $\delta(r)$ can be determined in tabular form by making physical measurements at intervals Δr over a finite range of r. Then $\Gamma(r)$ may be numerically determined from

$$\Gamma(r_k) \approx \frac{1}{r_n - r_k}\sum_{i=0}^{n-k+1} \delta(\tau_i)\,\delta(\tau_i + r_k)\,\Delta\tau_i \tag{6.31}$$

The difficulty with this result is that only the small portion of the curve about r = 0 may be used with confidence because of the finite range of r. Any attempt to fit the numerical curve by an analytic curve is complicated by the fact that any one of several equations seem to be a good fit.

There are three forms of correlation coefficients widely used throughout the literature:

$$\begin{aligned} &\text{(i)} \quad \rho(r) = e^{-r^2/\alpha^2} \ ; \\ &\text{(ii)} \quad \rho(r) = e^{-|r|/\alpha} \ ; \\ &\text{(iii)} \quad \rho(r) = e^{-|r|/\alpha}\cos br \ . \end{aligned} \tag{6.32}$$

where α and b are constants and r is the distance between points to be correlated. Form (i) is used in many theoretical studies, where some form of $\rho(r)$ must be assumed, because it

eases the labor of computation. The second form, (ii) is used when it seems to be a best fit to the numerical data while (iii) is sometimes used to extend the best fit range of (ii).

Many writers avoid the use of (ii) and (iii) because these forms have derivatives at r = 0 which differ from zero. This is possible only in the case when the ground height, $\zeta(r)$, is permitted to be a discontinuous function.[14] For this reason and ease of computation

$$\rho = e^{-r^2/\alpha^2} \tag{6.33}$$

is selected as the correlation coefficient to be used in the integrand. Here

r is the distance between points (or scatterers) to be correlated,

α is a measure of the distance between height-independent scatterers (or the correlation distance for scatterers).

From the geometry of Figure 6.1,

$$r = a\xi \tag{6.34}$$

where a is the radius of the sphere. Applying the law of cosines from spherical trigonometry

$$\cos\xi = \cos\theta_a \cos\theta_a' + \sin\theta_a \sin\theta_a' \cos\zeta \tag{6.35}$$

Using the first two terms of the Taylor's series for $\cos\xi$,

$$1 - \xi^2/2 \approx \cos\theta_a \cos\theta_a' + \sin\theta_a \sin\theta_a' \cos\zeta \tag{6.36}$$

with an error of less than 10% for $0 \leq \xi \leq 1.0$ radian. Thus

---

[14] Chernev, L. A., "Wave Propagation in a Random Medium," McGraw-Hill Book Co., 1960, Chapter 1.

$$\xi^2 \approx 2 - 2\cos\theta_a \cos\theta_a' - 2\sin\theta_a \sin\theta_a' \cos\zeta \tag{6.37}$$

and

$$r^2 \approx 2a^2 - 2a^2 \cos\theta_a \cos\theta_a' - 2a^2 \sin\theta_a \sin\theta_a' \cos\zeta \tag{6.38}$$

It is worthwhile to note that the approximation

$$\cos\xi \approx 1 - \frac{\xi^2}{2} \tag{6.39}$$

approximates the arc length r by its exact chord length. Applying the law of cosines to the triangle A'B'OA'

$$r_c^2 = 2a^2 - 2a^2 \cos\xi \tag{6.40}$$

where r_c is the chord A'B'. Utilizing the exact expression for $\cos\xi$,

$$r_c^2 = 2a^2 - 2a^2\cos\theta_a \cos\theta_a' - 2a^2 \sin\theta_a \sin\theta_a' \cos\zeta \tag{6.41}$$

Thus, if r is interpreted as a chord length, no approximation is necessary.

Substituting these results into the power return integral,

$$P_r = \mathcal{R}e \frac{a^2}{2(4\pi)^2 b^2} \iiint_A \iiint_{A'} \frac{P_T}{RR'} \cos\theta_i \cos\theta_i' \exp\left\{-j2ks\right.$$

$$\left. - 2k^2\sigma^2\left[\cos^2\theta_i + \cos^2\theta_i' - 2\cos\theta_i\cos\theta_i' \exp\left(-\frac{2a^2}{\alpha^2}\right.\right.\right.$$

$$\left.\left.\left. + \frac{2a^2}{\alpha^2}\cos\theta_a\cos\theta_a' + \frac{2a^2}{\alpha^2}\sin\theta_a\sin\theta_a'\cos\zeta\right)\right]\right\} dR\,d\varphi\,ds\,d\zeta \tag{6.42}$$

This integral is exact with the following assumptions:

(i) Huygen's-Kirchhoff integral can be applied;

(ii) the probability density of the rough surface is given by

$$p(\delta,\delta') = \frac{e^{-\frac{(\delta^2 + 2\rho\delta\delta' + \delta'^2)}{2\sigma^2(1-\rho^2)}}}{2\pi\sigma^2\sqrt{1-\rho^2}} \quad ;$$

(iii) the correlation coefficient, ρ, is

$$\rho = e^{-r^2/\alpha^2} .$$

By comparing Equation (6.42) to the integral developed by Moore and Williams, Equation (4.17) (specialized to the case of an isotropic antenna), the integral form of the scattering cross-section, $\sigma_o(\theta_i)$ is found to be

$$\sigma_o(\theta_i) = \frac{a R^2}{b\lambda^2}\cos\theta_i \int_{-(R_o-h)}^{R_o-R}\int_{-\pi}^{\pi}\int_{-\pi}^{\pi} \frac{\cos\theta_i'}{R'} \exp\Bigg\{-j2ks - 2k^2\sigma^2\Big[\cos^2\theta_i + \cos^2\theta_i' - 2\cos\theta_i\cos\theta_i' \exp\Big(-\frac{2a^2}{\alpha^2} + \frac{2a^2}{\alpha^2}\cos\theta_a\cos\theta_a' + \frac{2a^2}{\alpha^2}\sin\theta_a\sin\theta_a'\cos\zeta\Big)\Big]\Bigg\} d\phi\, d\zeta\, ds \quad . \tag{6.43}$$

$$\sigma_o(\theta_i) = \frac{2\pi a R^2}{b\lambda^2}\cos\theta_i \int_{-(R_o-h)}^{R_o-R}\int_{-\pi}^{\pi} \frac{\cos\theta_i'}{R'} \exp\Bigg\{-j2ks - 2k^2\sigma^2\Big[\cos^2\theta_i + \cos^2\theta_i' - 2\cos\theta_i\cos\theta_i' \exp\Big(-\frac{2a^2}{\alpha^2} + \frac{2a^2}{\alpha^2}\cos\theta_a\cos\theta_a' + \frac{2a^2}{\alpha^2}\sin\theta_a\sin\theta_a'\cos\zeta\Big)\Big]\Bigg\} d\zeta\, ds \quad . \tag{6.44}$$

Unfortunately, it appears that the remaining double integration must be carried out by machine methods. However, a different solution would be required for each different value of a/α, and each different ratio a/b which is inherently contained in the angles.

2. Evaluation of $\sigma_o(\theta_i)$ by Approximate Integration

The integral form of the scattering cross-section, as developed in the previous section, is mathematically exact within the given assumptions but not very useful. However, the integration can be performed after a few approximations and assumptions are made.

The scattering cross-section in terms of the correlation coefficient, ρ, is

$$\sigma_o(\theta_i) = \frac{a}{b}\frac{R^2}{\lambda^2}\cos\theta_i \iiint \frac{\cos\theta_i'}{R'} \exp\left[-j2ks - 2k^2\sigma^2\left(\cos^2\theta_i - 2\rho\cos\theta_i\cos\theta_i' + \cos^2\theta_i'\right)\right] d\Phi\, ds\, d\xi \quad (6.45)$$

If, as before, the correlation coefficient, ρ, is chosen to be e^{-r^2/α^2} and it is assumed that the integral converges rapidly for $r^2/\alpha^2 \ll 1$, then

$$\rho = e^{-r^2/\alpha^2} \approx 1 - \frac{r^2}{\alpha^2} \quad . \quad (6.46)$$

Davies' approximation for the distance r is[15]

$$r^2 \approx R^2\gamma^2 + s^2\csc^2\theta_i' \quad . \quad (6.47)$$

From spherical trigonometry,

$$\cos\gamma = \cos^2\theta_s + \sin^2\theta_s\cos\xi \quad . \quad (6.48)$$

---

[15] Davies, H., op. cit.

Approximating $\cos\gamma$ by the first two terms of its series expansion, it is found that

$$\gamma^2 \approx 2\sin^2\theta_s(1-\cos\zeta) \ . \tag{6.49}$$

Thus

$$r^2 \approx 2R^2\sin^2\theta_s - 2R^2\sin^2\theta_s\cos\zeta + s^2\csc^2\theta_i' \ . \tag{6.50}$$

The integral form of the scattering cross-section now becomes

$$\sigma_s(\theta_i) \approx \mathrm{Re}\ \frac{aR^2}{b\lambda^2}\cos\theta_i \iiint \frac{\cos\theta_i'}{R'}\ \exp\Big\{-j2ks$$

$$-2k^2\sigma^2\Big[\cos^2\theta_i + \cos^2\theta_i' + 2\cos\theta_i\cos\theta_i'\Big(-1$$

$$+\frac{2R^2}{\alpha^2}\sin^2\theta_s - \frac{2R^2}{\alpha^2}\sin^2\theta_s\cos\zeta$$

$$+ s^2\csc^2\theta_i'\Big)\Big]\Big\}\ d\varphi\ ds\ d\zeta \ . \tag{6.51}$$

The limits on the integration are

$$-\pi \le \varphi \le \pi$$

$$-\pi \le \zeta \le \pi \qquad (6.52)$$

$$-(R-h) \le s \le (R_o-h),$$

where R_o is the maximum range within the irradiated region.

The integration on φ presents no problem;

$$\int_{-\pi}^{\pi} d\varphi = 2\pi \quad . \qquad (6.53)$$

The ζ integral can be rearranged in a form which has a tabulated result.

$$\int_{-\pi}^{\pi} e^{\frac{8k^2\sigma^2R^2}{\alpha^2}\cos\theta_i\cos\theta_i'\sin^2\theta_s\cos\zeta}\, d\zeta$$

$$= 2\int_{0}^{\pi} e^{\frac{8k^2\sigma^2R^2}{\alpha^2}\cos\theta_i\cos\theta_i'\sin^2\theta_s\cos\zeta}\, d\zeta$$

$$= 2\pi\, I_o\left[\frac{8k^2\sigma^2R^2\cos\theta_i\cos\theta_i'\sin^2\theta_s}{\alpha^2}\right], \qquad (6.54)$$

where I_o is the modified Bessel function of the first kind.

The s integration is of the form

$$\int_{-(R-h)}^{R_o-h} \frac{\cos\theta_i'}{R'} I_o[\Lambda\cos\theta_i'] \exp\left[-j2ks - 2k^2\sigma^2(\cos\theta_i - \cos\theta_i')^2\right.$$

$$\left. - \Lambda\cos\theta_i' - \frac{4k^2\sigma^2}{\alpha^2} s^2\cos\theta_i\cos\theta_i'\csc^2\theta_i'\right] ds \qquad (6.55)$$

where

$$\Lambda = \frac{8k^2\sigma^2R^2}{\alpha^2}\cos\theta_i\sin^2\theta_s \qquad (6.56)$$

and θ_i' is a function of s. If it is assumed that the integral converges rapidly with the explicit s, the approximation $\theta_i \approx \theta_i'$ may be used with great advantage. The integral then becomes

$$\frac{\cos\theta_i}{R} I_o[\Lambda\cos\theta_i]\, e^{-\Lambda\cos\theta_i}\int_{-(R-h)}^{R_o-R} e^{-j2ks - \left(\frac{4k^2\sigma^2\cot^2\theta_i}{\alpha^2}\right)s^2} ds \qquad (6.57)$$

Cooper has shown that an integral of this form converges so rapidly that the finite limits, -(R-h) and (R_o-R), may be extended to $-\infty$ and $+\infty$ respectively with very little error in the final result.[16] This also seems to lend more weight to the validity of the approximation $\theta_i \approx \theta_i'$. From the integral tables

$$\int_{-\infty}^{\infty} e^{-j2ks - \left(\frac{4k^2\sigma^2\cot^2\theta_i}{\alpha^2}\right)s^2} ds = \frac{\alpha\sqrt{\pi}}{2k\sigma}\tan\theta_i\, e^{-\frac{\alpha^2}{4\sigma^2}\tan^2\theta_i} \qquad (6.58)$$

---

[16] Cooper, J. A., "Comparison of Observed and Calculated Near-Vertical Radar Ground Return Intensities and Fading Spectra," Tech. Report EE-10, Univ. of New Mexico, Eng. Exp. Station, May 1958.

Thus

$$\int_{-(R-h)}^{(R_o-R)} \frac{\cos\theta_i'}{R} I_o[\Lambda\cos\theta_i'] \exp\Big[-j2ks - 2k^2\sigma^2(\cos\theta_i - \cos\theta_i')^2 - \Lambda\cos\theta_i' - \frac{4k^2\sigma^2}{\alpha^2} s^2\cos\theta_i\cos\theta_i'\csc^2\theta_i'\Big] ds$$

$$\approx \frac{\alpha\sqrt{\pi}}{2k\sigma R}\sin\theta_i I_o[\Lambda\cos\theta_i] e^{-\Lambda\cos\theta_i - \frac{\alpha^2}{4\sigma^2}\tan^2\theta_i} . \qquad (6.59)$$

From Figure 6.1 and the law of sines,

$$\sin\theta_s = \frac{a}{b}\sin\theta_i . \qquad (6.60)$$

Combining the results of the integrations,

$$\sigma_o(\theta_i) \approx \frac{\pi^{5/2} a\alpha R}{kb\sigma\lambda^2}\sin 2\theta_i I_o\left[\frac{2k^2\sigma^2a^2R^2}{\alpha^2 b^2}\sin^2 2\theta_i\right] \cdot e^{-\frac{\alpha^2}{4\sigma^2}\tan^2\theta_i - \frac{2k^2\sigma^2a^2R^2}{\alpha^2b^2}\sin^2 2\theta_i} . \qquad (6.61)$$

This result can be simplified by using the asymptotic form of the modified Bessel function,

$$I_n(x) \approx \frac{e^x}{\sqrt{2\pi x}} \quad , \; x \to \infty . \qquad (6.62)$$

$I_o(x)$ and $e^x(2\pi x)^{-1/2}$ are graphed in Figure 6.2 which shows that x does not have to be very large to obtain a reasonably good approximation. It will be assumed that

$$I_o(x) \approx \frac{e^x}{\sqrt{2\pi x}} \quad , \; x \geq 2 . \qquad (6.63)$$

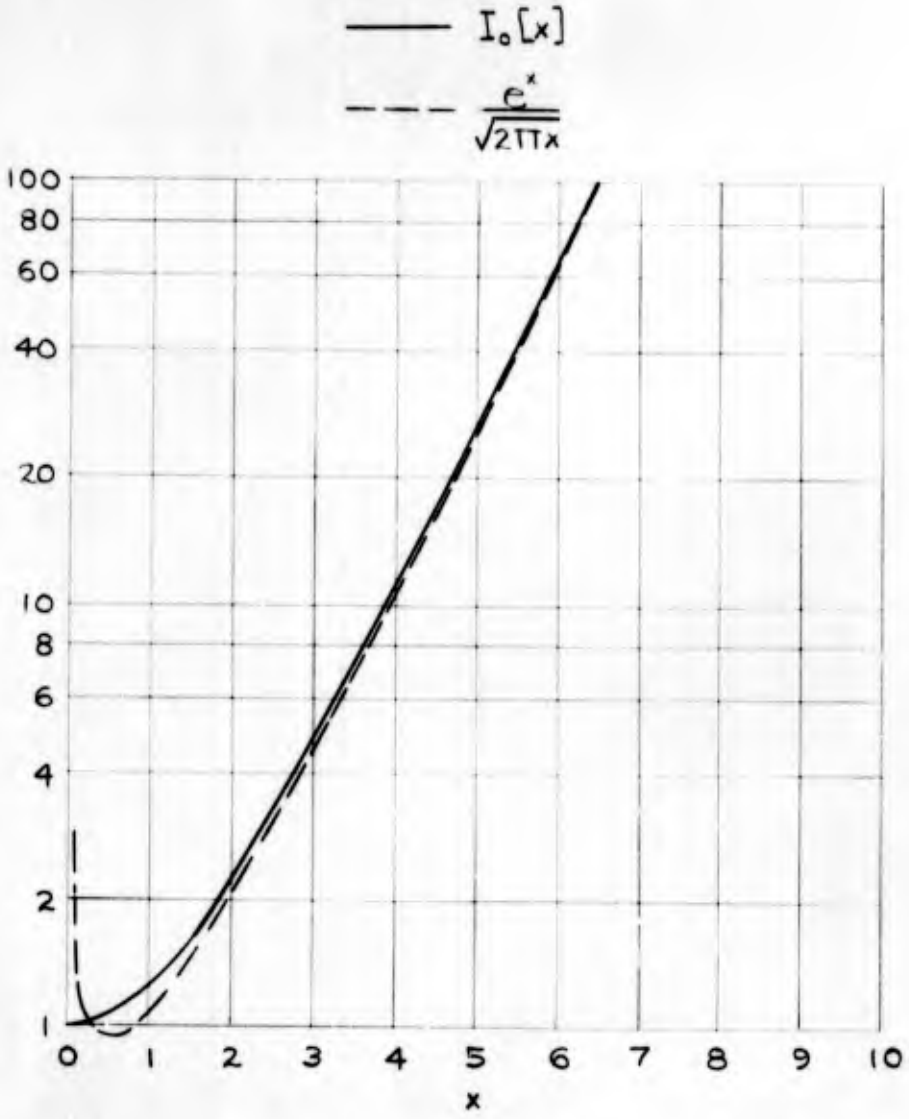

Figure 6.2

Thus,

$$\sigma_o(\theta_i) \approx \frac{\alpha^2}{8\sigma^2} e^{-\frac{\alpha^2}{4\sigma^2}\tan^2\theta_i} \quad , \frac{2k^2\sigma^2a^2}{\alpha^2 b^2}\sin^2 2\theta_i \geq 2 \; . \tag{6.64}$$

At $\theta_i = 0^\circ$, $\sin 2\theta_i = 0$ and $I_o[0] = 1$, which implies $\sigma_o(0^\circ) = 0$; however, this is an erroneous result of the approximations for the distance r.

If the integral form of the scattering cross-section is written using all the approximations and assumptions previously made except the approximation for the distance r, the result is

$$\sigma_o(\theta_i) \approx \mathrm{Re}\,\frac{aR}{b\lambda^2}\cos^2\theta_i \iiint e^{-j2ks-\left(\frac{4k^2\sigma^2}{\alpha^2}\cos^2\theta_i\right)r^2} d\varphi ds d\xi \; . \tag{6.65}$$

Evaluating this expression at $\theta_i = 0^\circ$,

$$\sigma_o(0^\circ) \approx \mathrm{Re}\,\frac{ah}{b\lambda^2} \iiint e^{-j2ks-\frac{4k^2\sigma^2}{\alpha^2}r^2} d\varphi ds d\xi \; . \tag{6.66}$$

A limited range for $\sigma_o(0^\circ)$ can be found by making use of inequalities.

From Figure 6.3

$$r^2 = (h+s)^2 + h^2 - 2h(h+s)\cos\theta_s' \quad , \theta_i = 0^\circ \; , \tag{6.67}$$

from which it is immediately apparent that

$$r^2 \geq s^2 \; . \tag{6.68}$$

Also, by the law of cosines,

$$\cos\theta_s' = \frac{b^2 - a^2 + (h+s)^2}{2b(h+s)} \tag{6.69}$$

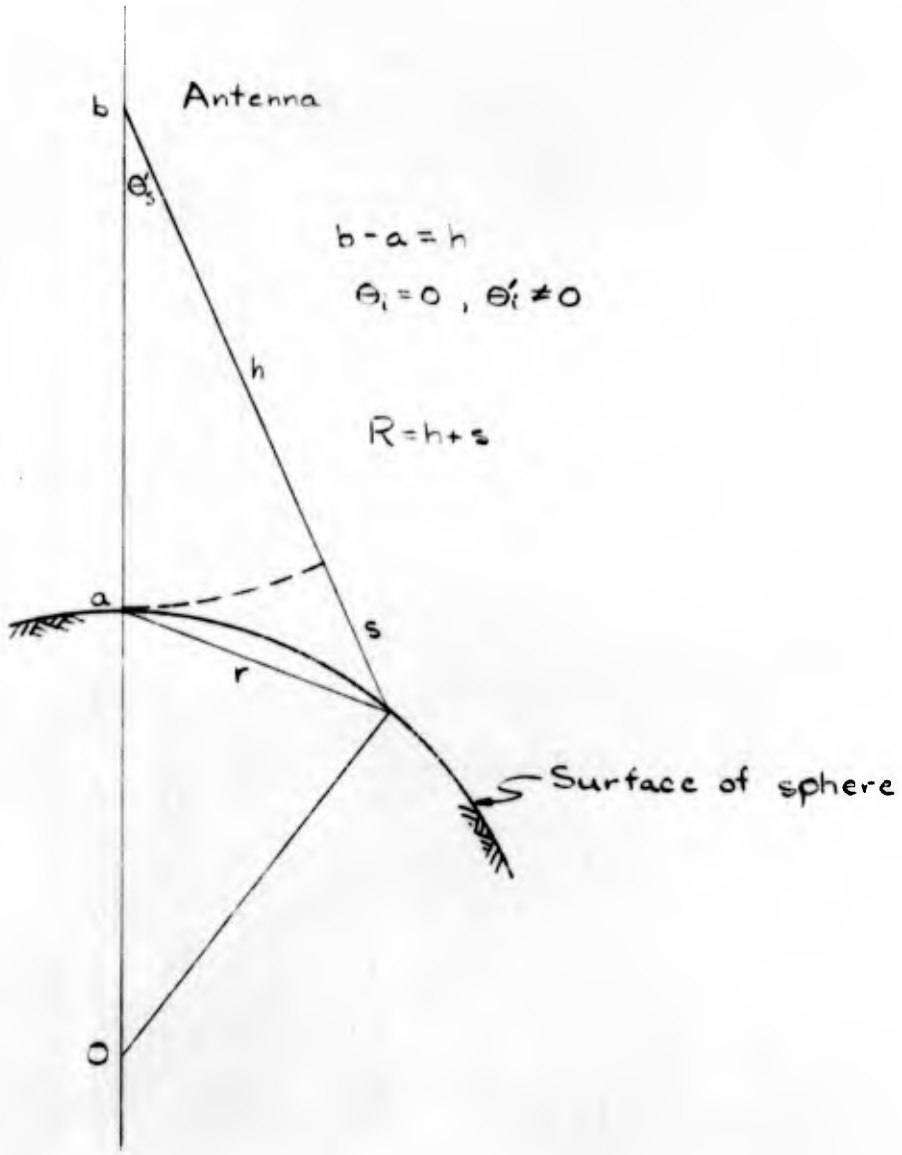
b
Antenna
θ_i'
b - a = h
$\theta_i = 0$, $\theta_i' \neq 0$
h
R = h + s
a
s
r
Surface of sphere
O

Figure 6.3

Combining these results,

$$r^2 = \frac{2hs + s^2}{1 + h/a} \leq \frac{2hs + r^2}{1 + h/a} \tag{6.70}$$

as $r^2 \geq s^2$. Solving the inequality for r^2,

$$r^2 \leq 2as \,. \tag{6.71}$$

For the other inequality

$$r^2 = \frac{2hs + s^2}{1 + h/a} \geq \frac{2hs}{1 + h/a} = \frac{2ahs}{b} \,. \tag{6.72}$$

As the inequalities on r^2 are independent of φ and ξ,

$$\sigma_o(0°) \approx \frac{(2\pi)^2 ah}{b\lambda^2} \int_0^{R_o - h} e^{-j2ks - \frac{4k^2\sigma^2 r^2}{\alpha^2}} ds \,. \tag{6.73}$$

Here again it will be assumed that R_o-h is so large that the upper limit may be replaced with infinity. Now as

$$\frac{2ahs}{b} \leq r^2 \leq 2as \,, \tag{6.74}$$

then

$$e^{-2as} \leq e^{-r^2} \leq e^{-\frac{2ahs}{b}} \,. \tag{6.75}$$

Making use of the theorem that if $f(x) \leq g(x)$ on the interval $[a,b]$, then

$$\int_a^b f(x)\,dx \leq \int_a^b g(x)\,dx \,,$$

$\sigma_o(0°)$ is found to be between the extremes

$$\frac{(2\pi)^2 ah}{b\lambda^2} \int_0^\infty (\cos 2ks)\, e^{-\frac{8k^2\sigma^2 a}{\alpha^2} s}\, ds \quad (\leq) \quad \sigma_o(0°)$$

$$(\leq) \quad \frac{(2\pi)^2 ah}{b\lambda^2} \int_0^\infty (\cos 2ks)\, e^{-\frac{8k^2\sigma^2 ah}{\alpha^2 b}}\, ds \,. \tag{6.76}$$

Here the inequalities are placed in parentheses as a reminder that the integrals are approximations. Integrating on s,

$$\frac{(2\pi)^2 ah}{b\lambda^2}\ \frac{8k^2\sigma^2 a}{\alpha^2}\left[\left(\frac{8k^2\sigma^2 a}{\alpha^2}\right)^2+4k^2\right]^{-1}(\leq)\ \sigma_0(0^0)$$

$$(\leq)\ \frac{(2\pi)^2 ah}{b\lambda^2}\ \frac{8k^2\sigma^2 ah}{\alpha^2 b}\left[\left(\frac{8k^2\sigma^2 ah}{\alpha^2 b}\right)^2+4k^2\right]^{-1}, \tag{6.77}$$

or

$$\frac{(2\pi)^2 ah}{b\lambda^2}\ \frac{2\sigma^2 a}{\alpha^2}\left[\left(\frac{4k\sigma^2 a}{\alpha^2}\right)^2+1\right]^{-1}\ (\leq)\ \sigma_0(0^0)$$

$$(\leq)\ \frac{(2\pi)^2 ah}{b\lambda^2}\ \frac{2\sigma^2 ah}{\alpha^2 b}\left[\left(\frac{4k\sigma^2 ah}{\alpha^2 b}\right)^2+1\right]^{-1}. \tag{6.78}$$

In the denominators of the extremes note that

$$\left[\left(\frac{4k\sigma^2 a}{\alpha^2}\right)^2+1\right]^{-1} < \left[\left(\frac{4k\sigma^2 ah}{\alpha^2 b}\right)^2+1\right]^{-1} \tag{6.79}$$

as $h/b < 1$, and if

$$\left(\frac{4k\sigma^2 ah}{\alpha^2 b}\right)^2 >> 1, \tag{6.80}$$

then the (+1) term may be dropped as a further approximation. Thus

$$\frac{\alpha^2}{8b\sigma^2}\ (\leq)\ \sigma_0(0^0)\ (\leq)\ \frac{\alpha^2}{8\sigma^2} \tag{6.81}$$

approximately. As the expression

$$\sigma_0(\theta_i) = \frac{\alpha^2}{8\sigma^2}\, e^{-\frac{\alpha^2}{4\sigma^2}\tan^2\theta_i}, \quad \frac{2k^2\sigma^2 a^2 R^2}{\alpha^2 b^2}\sin^2 2\theta_i \geq 2 \tag{6.82}$$

is not dependent on altitude or the sphere radius when its inequality is satisfied, there is little reason to believe $\sigma_o(0^o)$ is dependent on altitude and sphere radius. Hence, it will be assumed that

$$\sigma_o(\theta_i) \approx \frac{\alpha^2}{8\sigma^2} e^{-\frac{\alpha^2}{4\sigma^2}\tan^2\theta_i}, \quad \frac{2k^2\sigma^2a^2R^2}{\alpha^2 b^2}\sin^2 2\theta_i \geq 0 \tag{6.83}$$

where

α is a measure of the distance between height independent scatterers,

σ is the standard deviation of the scatterers about the mean radius of the sphere.

In general, the quantities α and σ, or α/σ, are very difficult to determine for a given radar target. One method of determining the ratio α/σ is to make measurements of the power returned to a radar from the actual target. Another method is to compute α and σ from a contour map. The accuracy of the latter method is limited by the closeness of contours.

It should be remembered that the above expression for $\sigma_o(\theta_i)$ is an approximation and just one of several theoretical scattering cross-sections which may exist. A different scattering cross-section can be obtained with a different surface roughness model and/or a different correlation coefficient.

By an analysis very similar to the one given in this Chapter, it can be shown that Equation (6.83) is the approximate scattering cross-section for a rough plane. The mathematical details of development are given in Appendix B.

CHAPTER VII

CALCULATED EXAMPLES OF POWER RETURN

Examples of the median power return pulse from the earth's surface are calculated at altitudes of 6.38, 159, 319, and 638 km. These altitudes are approximately 4,100, 200, and 400 miles respectively.

For the radar system it is assumed that

$$P_T(d) = \begin{cases} P_{T_0} & , \ 0 \le d \le \tau \\ 0 & , \ \tau \le d \end{cases}$$
$$G(\theta_s) = \begin{cases} G_0 & , \ 0 \le \theta_s \le \pi/2 \\ 0 & , \ \pi/2 < \theta_s \end{cases} \qquad (7.1)$$

where τ is the transmitted pulse length and θ_s is the antenna angle from the vertical. The radar cross-section of the earth's surface is assumed to be that which was previously derived:

$$\sigma_0(\theta_i) \approx \frac{\alpha^2}{8\sigma^2} e^{-\frac{\alpha^2}{4\sigma^2}\tan^2\theta_i} , \ \theta_i \ge 0 . \qquad (7.2)$$

The following values of x^2K^2, $(1-x^2)\beta$, and α^2/σ^2 were chosen for the calculation of the power return:

$$\begin{aligned} &\text{(i)} \quad x^2K^2 = 0, \ (1-x^2)\beta = 0.13, \ \alpha^2/\sigma^2 = 32; \\ &\text{(ii)} \quad x^2K^2 = 0.10, \ (1-x^2)\beta = 0.24, \ \alpha^2/\sigma^2 = 60; \\ &\text{(iii)} \quad x^2K^2 = 0.55, \ (1-x^2)\beta = 0.25, \ \alpha^2/\sigma^2 = 100. \end{aligned} \qquad (7.3)$$

These are experimentally determined values obtained with a 415 mc. radar at altitudes between 4,000 and 12,000 feet.[17]

---

[17] Edison, A. R., Moore, R. K., and Warner, B. D., "Radar Terrain Return Measured at Near-Vertical Incidence," Trans.I.R.E P.G.A.P. Vol. AP-8, No. 3, May 1960, pp. 246-54.

The first set of values are approximately those determined for forests, the second set approximately applies to cities and farmland, and the third set are approximately those determined for water.

There is very little doubt as to the validity of these numbers at the higher altitudes; the question is "to what targets may these numbers be applied?" It is highly improbable that they apply to the same targets at these high altitudes as they do at the low altitudes.

The results of the calculations are shown graphically in Figures 7.1, 7.2, 7.3, and 7.4. As the transmitted pulse length, τ, was assumed to be 10 μ seconds, this is also the duration of the specular power return as shown in Figures 7.1, 7.3, and 7.4. The square appearance of these curves is a result of using a square transmitted pulse; however, this points out the manner in which specular and scatter power combine. If a transmitted pulse with a continuous first derivative had been used, the combination of specular and scatter power would have a continuous first derivative.

The power return pulses shown in these figures are median (50 percentile) values. The range of fading given for a particular pulse was determined experimentally and defines the

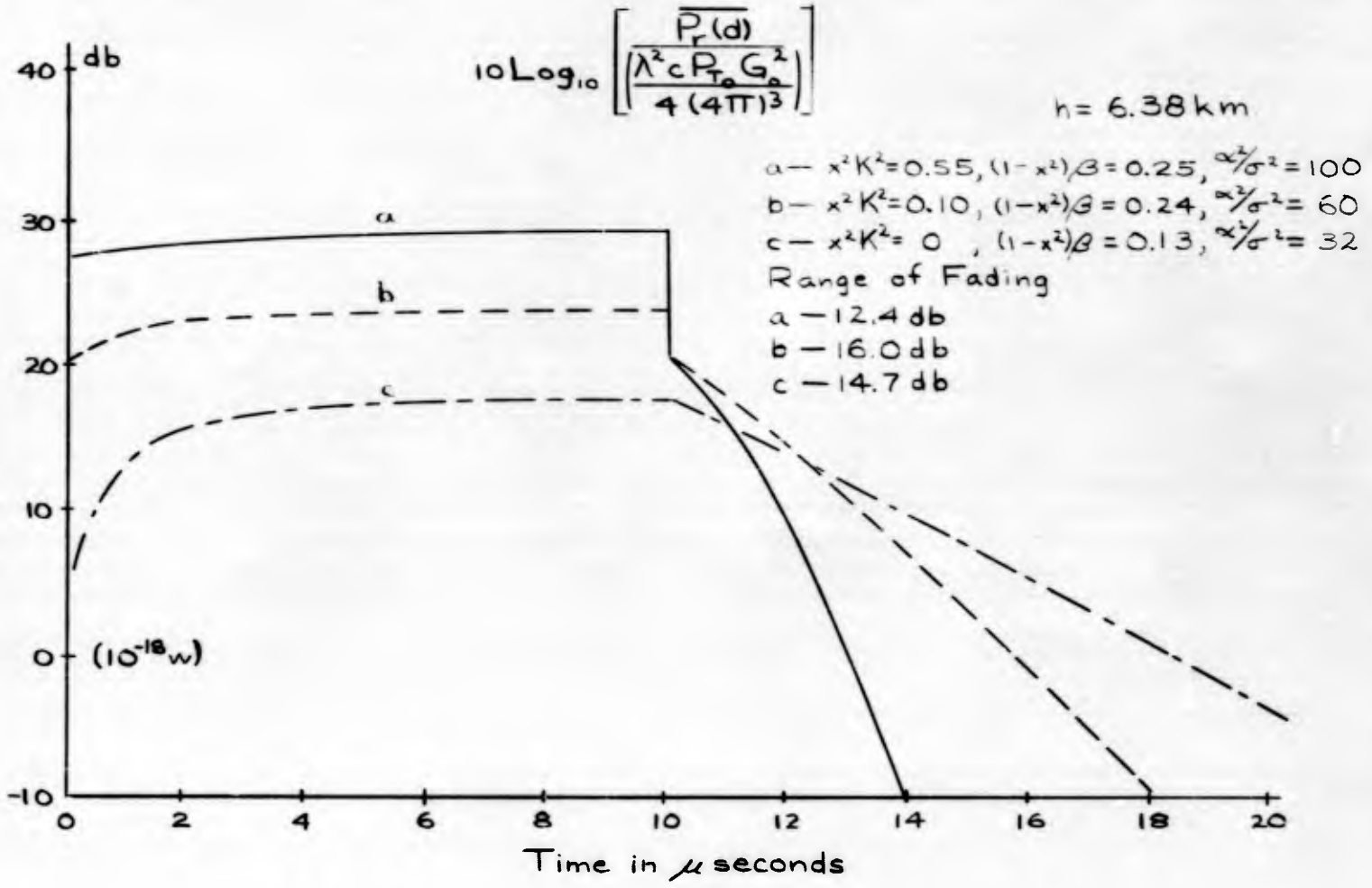
$10 \text{Log}_{10} \left[\frac{\overline{P_r(d)}}{\frac{\lambda^2 c P_{T_o} G_o^2}{4(4\pi)^3}} \right]$
h = 6.38 km
a — $x^2K^2 = 0.55$, $(1-x^2)\beta = 0.25$, $\alpha^2/\sigma^2 = 100$
b — $x^2K^2 = 0.10$, $(1-x^2)\beta = 0.24$, $\alpha^2/\sigma^2 = 60$
c — $x^2K^2 = 0$, $(1-x^2)\beta = 0.13$, $\alpha^2/\sigma^2 = 32$
Range of Fading
a — 12.4 db
b — 16.0 db
c — 14.7 db
db
40
30
20
10
0
-10
$(10^{-18}w)$
a
b
c
0
2
4
6
8
10
12
14
16
18
20
Time in μ seconds

Figure 7.1

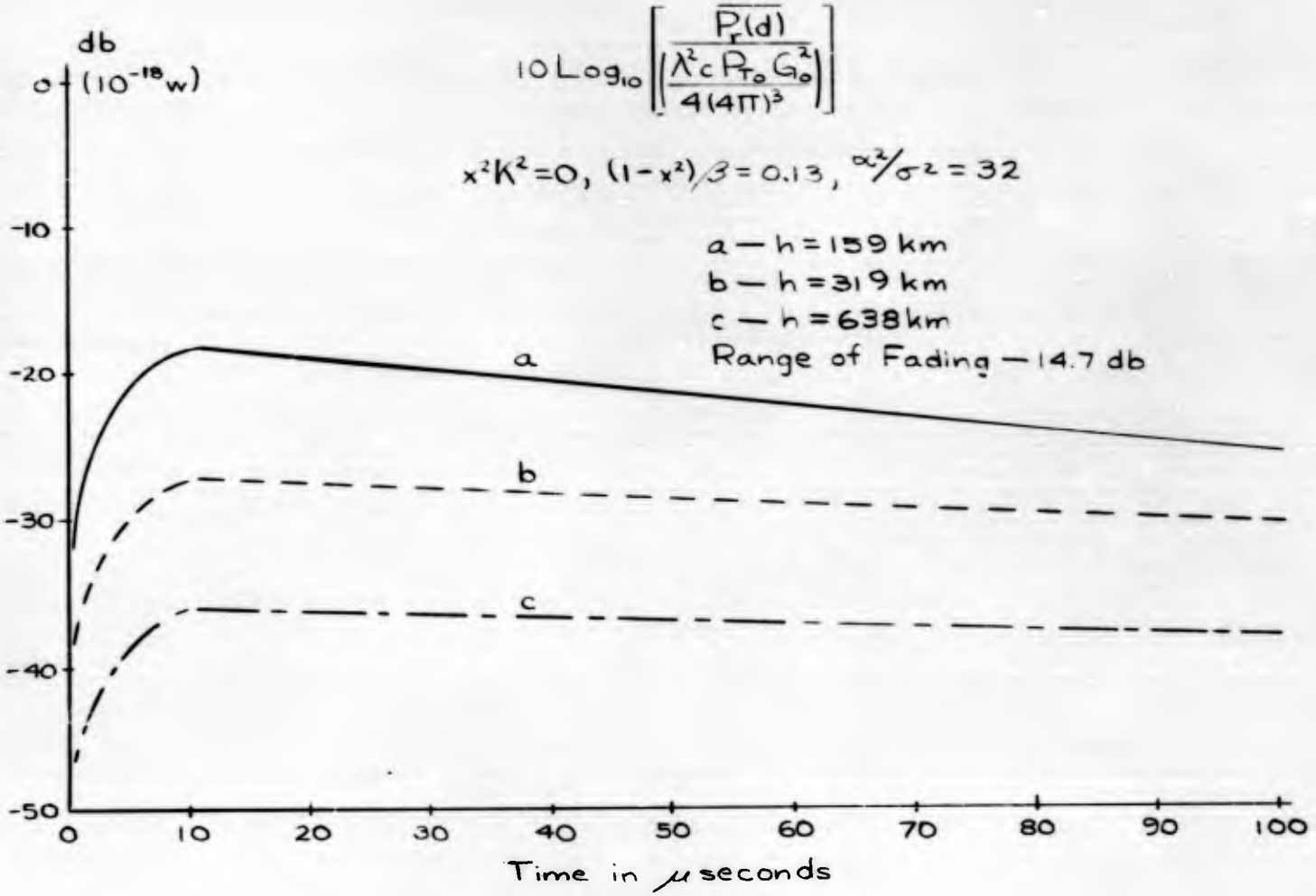
db
(10⁻¹⁸ w)
0
-10
-20
-30
-40
-50
$10 \log_{10}\left[\frac{\overline{P_r(d)}}{\left(\frac{\lambda^2 c P_{T_0} G_0^2}{4(4\pi)^3}\right)}\right]$
$x^2K^2=0,\ (1-x^2)/\beta=0.13,\ \alpha^2/\sigma^2=32$
a — h = 159 km
b — h = 319 km
c — h = 638 km
Range of Fading — 14.7 db
a
b
c
0
10
20
30
40
50
60
70
80
90
100
Time in μ seconds

Figure 7.2

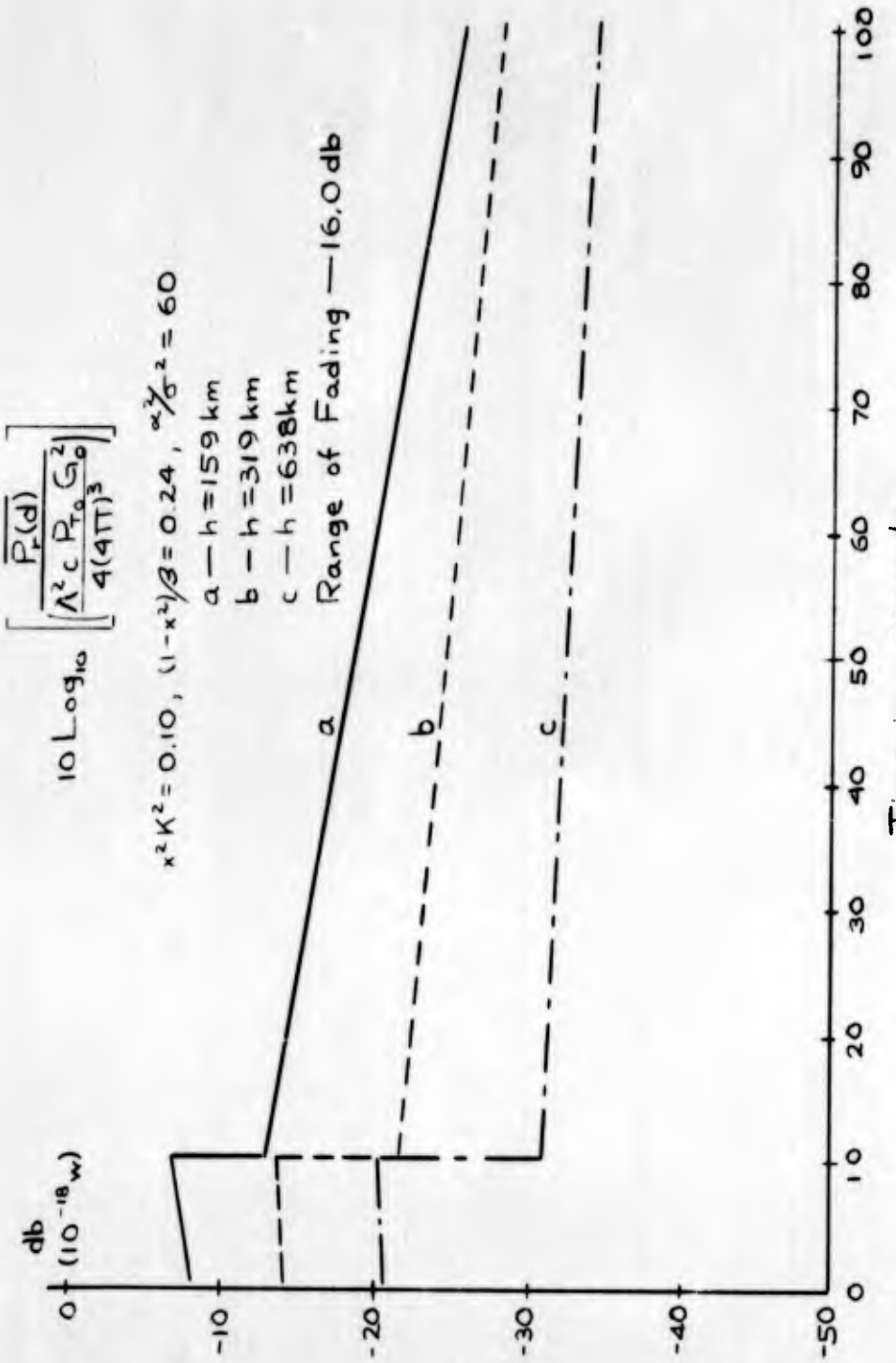
10 Log10 [P̄r(d) / (λ²c PTo Go² / 4(4π)³)]
x²K² = 0.10, (1-x²)/3 = 0.24, α²/σ² = 60
a — h = 159 km
b — h = 319 km
c — h = 638 km
Range of Fading — 16.0 db
db (10⁻¹⁸ w)
0
-10
-20
-30
-40
-50
0
10
20
30
40
50
60
70
80
90
100
Time in μ seconds
a
b
c

Figure 7.3

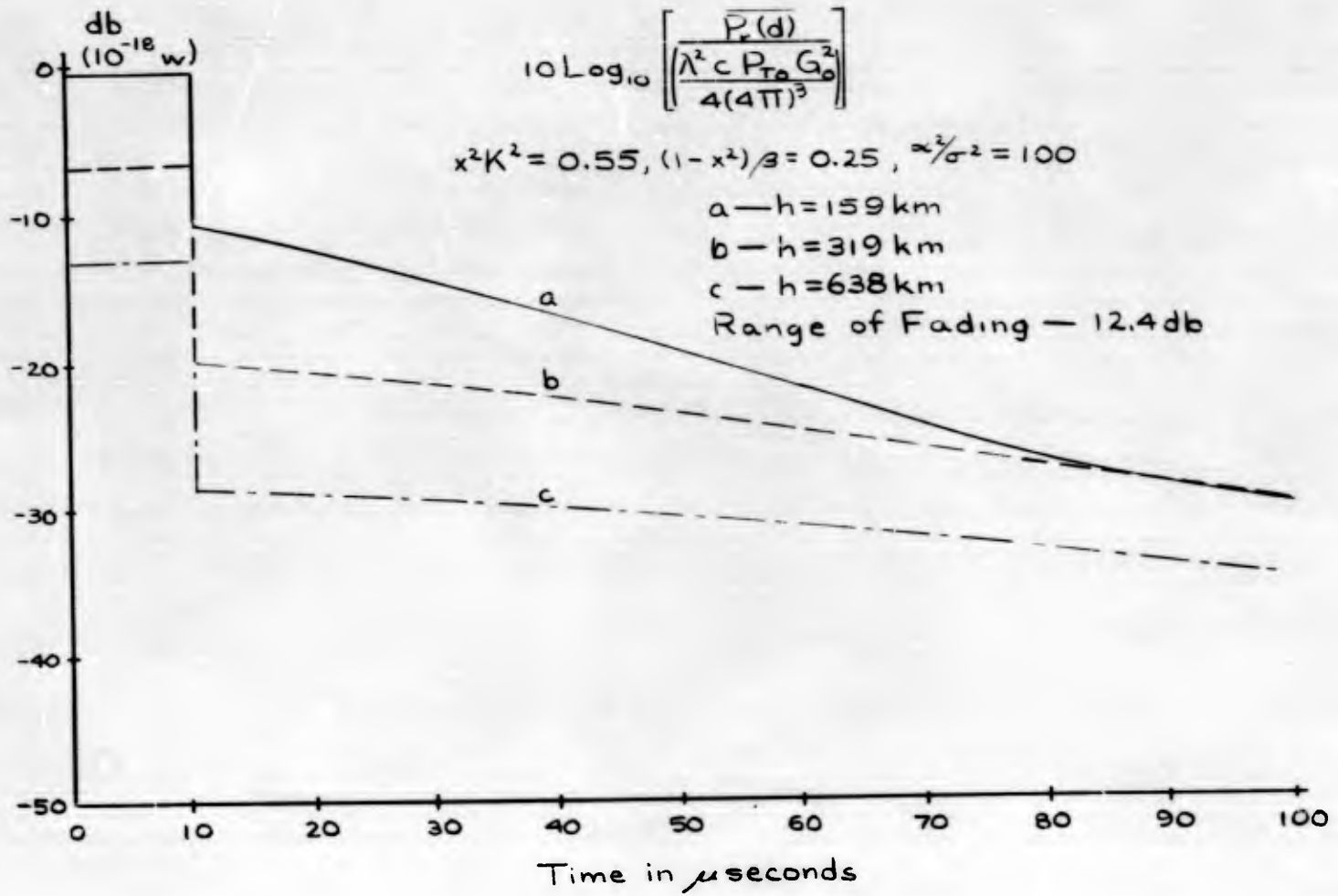
db
(10^-18 w)
0
-10
-20
-30
-40
-50
$10 \text{Log}_{10}\left[\frac{\overline{P_r(d)}}{\frac{\lambda^2 c P_{To} G_o^2}{4(4\pi)^3}}\right]$
$x^2K^2 = 0.55, (1-x^2)/\beta = 0.25, \alpha^2/\sigma^2 = 100$
a — h = 159 km
b — h = 319 km
c — h = 638 km
Range of Fading — 12.4 db
a
b
c
0
10
20
30
40
50
60
70
80
90
100
Time in μ seconds

Figure 7.4

range within which 90% of the return power will found; i.e., the range of fading is the difference between the 95 and 5 percentile curves. The exact location of the 5 and 95 percentile curves with respect to the 50 percentile curve is slightly variant in the experimental results and therefore not reported here. The range of fading is included to emphasize the fact that it is quite unlikely that any individual return pulse will appear as those shown.

A different analytic form of the scattering cross-section has been derived by assuming a correlation coefficient of the form

$$\rho = e^{-|r|/\alpha} \tag{7.4}$$

and the probability density function[18]

$$p(\delta,\delta') = \frac{e^{-\frac{(\delta^2 + 2\rho\delta\delta' + \delta'^2)}{2\sigma^2(1-\rho^2)}}}{2\pi\sigma^2\sqrt{1-\rho^2}} \tag{7.5}$$

This probability density is the same as that given in Equation (6.22). The resultant scattering cross-section is of the form

$$\sigma_0(\theta_i) \approx \frac{4\pi\sqrt{2}\,\alpha^2\,\theta_i \cos\theta_i \cot\theta_i\, e^{-4k^2\sigma^2\cos^2\theta_i}}{\lambda^2} \cdot \sum_{n=1}^{\infty} \frac{(4k^2\sigma^2\cos^2\theta_i)^n}{(n-1)!\left[2k\alpha^2\sin^2\theta_i + n^2\right]^{3/2}} \tag{7.6}$$

Examples of the power returned from the above expression for scattering cross-section were calculated for the following scattering parameters:

---

[18] Hayre, H. S., and Moore, R. K., "Theoretical Scattering Coefficients for the Near-Vertical Incidence from Contour Maps," accepted for publication in J. Res. Nat. Bur. Stand., Vol. 65 D.

(i) $x^2k^2 = 0.10$, $(1-x^2)\beta = 0.24$. $\alpha/\lambda = 1$, $\sigma/\lambda = 0.1$, $\alpha^2/\sigma^2 = 100$

(ii) $x^2k^2 = 0.55$, $(1-x^2)\beta = 0.25$. $\alpha/\lambda = 2$, $\sigma/\lambda = 0.05$, $\alpha^2/\sigma^2 = 1600$

(7.8)

These values result in scattering curves which are approximately the same as (7.3 ii) and (7.3 iii), respectively, at zero angle of incidence.

The calculated return power is shown in Figures 7.5, 7.6, and 7.7. Here the scatter power drops off more rapidly than that shown in Figures 7.1, 7.3, and 7.4; otherwise, the return power is comparable.

A study of Equation (5.1) shows the specular power varies as h^{-2} while the scatter power varies more nearly as h^{-3}. Thus, the ratio

$$\frac{\text{Specular Power}}{\text{Scatter Power}} \propto h \quad . \tag{7.9}$$

This ratio was evaluated at t = 10 μseconds for the return power shown in Figures 7.1, 7.3, 7.4, 7.5, 7.6, and 7.7. The result is shown in Figure 7.8. Each of these examples represents a quite smooth surface. A 10 $\log_{10} h$ curve is plotted through the end point of each of the power ratio curves to show how rapidly the power ratio is approaching the h variation. Once again, it is emphasized that these curves are plotted for a target which always appears to be the same at any radar altitude. The difference in shape between any two power ratio curves can be attributed to the differences of their respective scattering cross-sections.

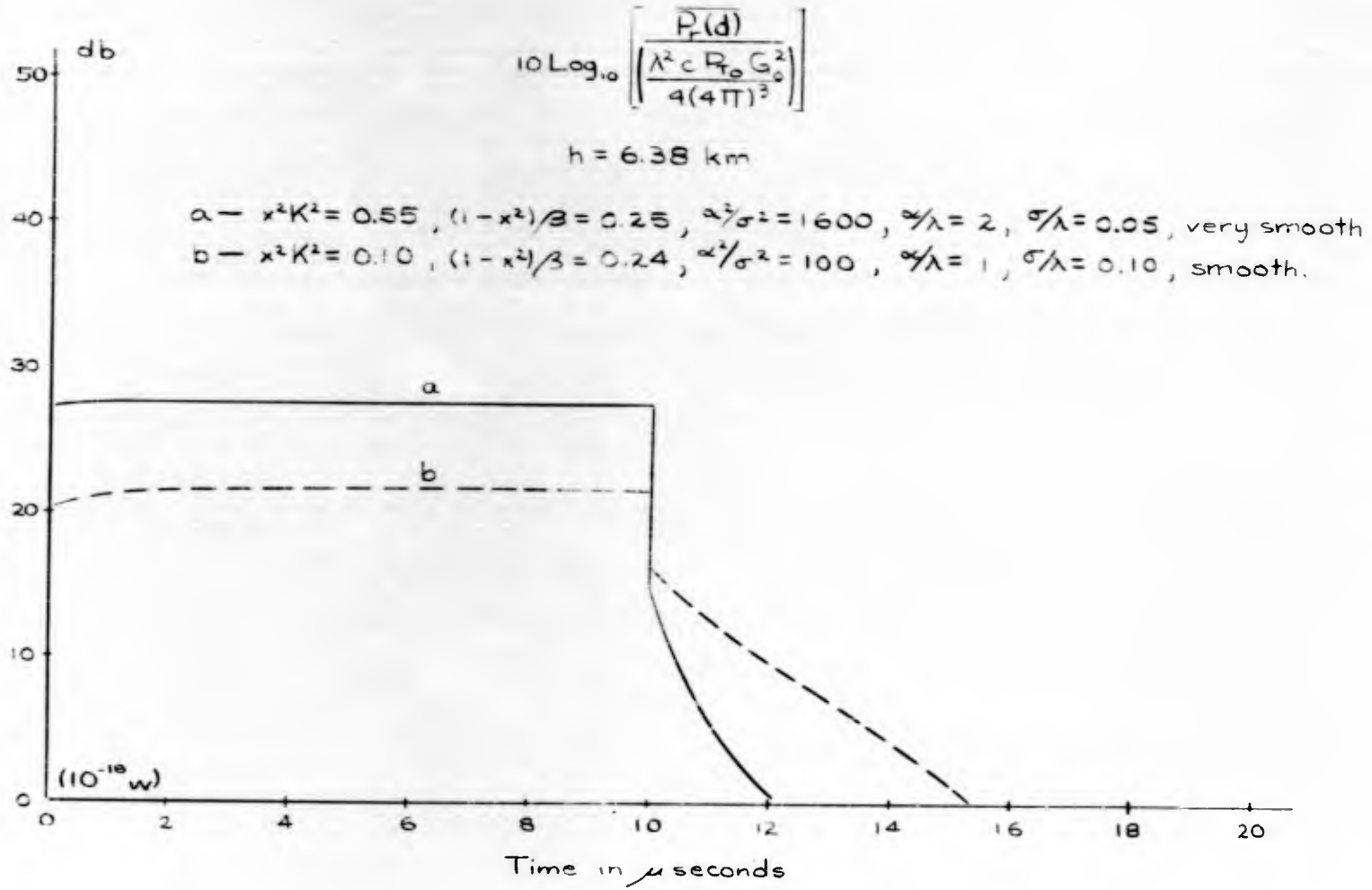
$10\,Log_{10}\left[\frac{\overline{P_r(d)}}{\left(\frac{\lambda^2 c P_{T_0} G_0^2}{4(4\pi)^3}\right)}\right]$
h = 6.38 km
a — $x^2K^2 = 0.55$, $(1-x^2)/\beta = 0.25$, $\alpha^2/\sigma^2 = 1600$, $\alpha/\lambda = 2$, $\sigma/\lambda = 0.05$, very smooth
b — $x^2K^2 = 0.10$, $(1-x^2)/\beta = 0.24$, $\alpha^2/\sigma^2 = 100$, $\alpha/\lambda = 1$, $\sigma/\lambda = 0.10$, smooth.
db
50
40
30
20
10
0
a
b
$(10^{-18}$ w)
0
2
4
6
8
10
12
14
16
18
20
Time in μ seconds

Figure 7.5

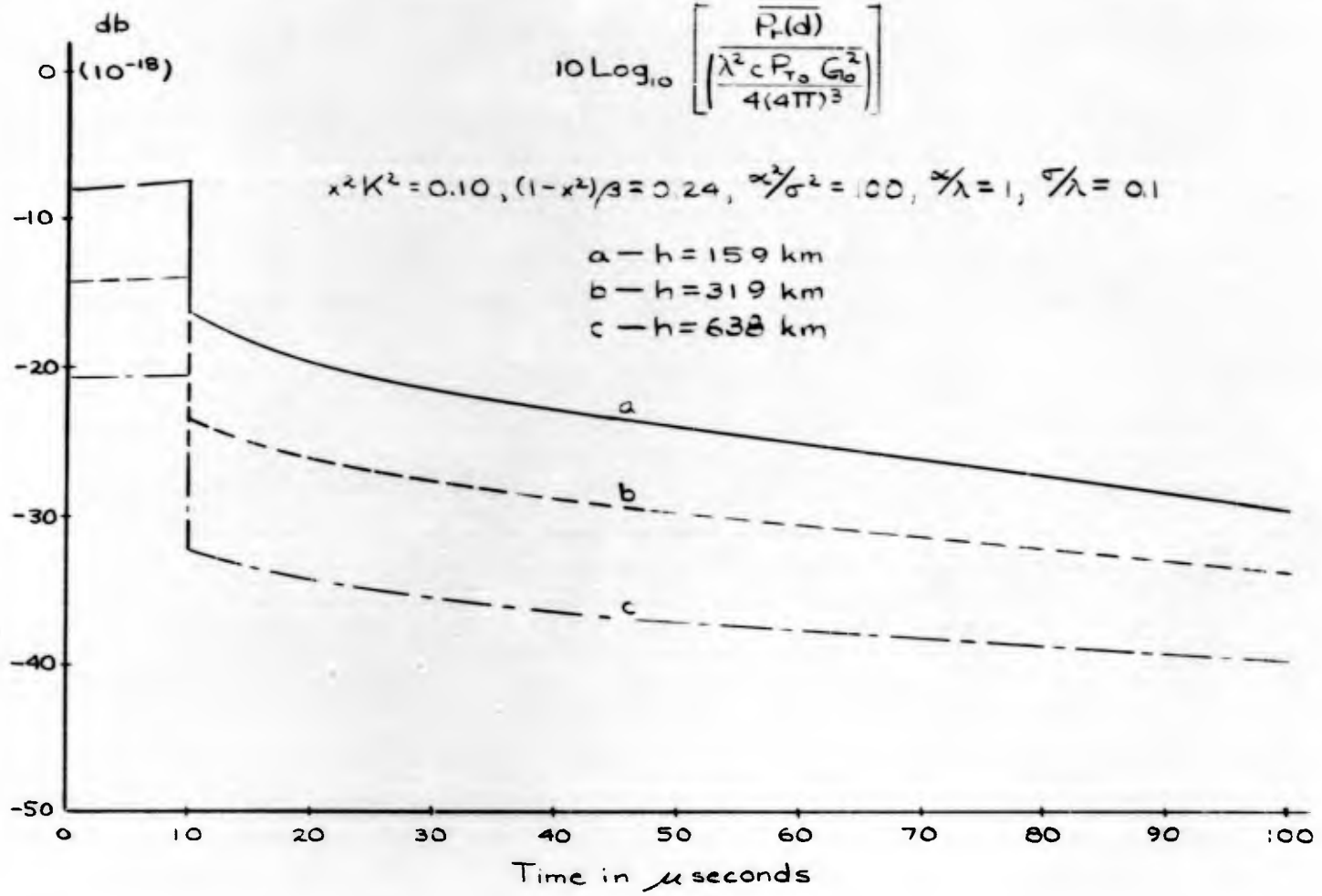
db
(10⁻¹⁸)
0
-10
-20
-30
-40
-50
$10 \log_{10} \left[\frac{\overline{P_r(d)}}{\frac{\lambda^2 c P_{T_0} \overline{G_0^2}}{4(4\pi)^3}} \right]$
$x^2K^2 = 0.10$, $(1-x^2)/\beta = 0.24$, $\alpha^2/\sigma^2 = 100$, $\alpha/\lambda = 1$, $\sigma/\lambda = 0.1$
a — h = 159 km
b — h = 319 km
c — h = 638 km
a
b
c
0
10
20
30
40
50
60
70
80
90
100
Time in μ seconds

Figure 7.6

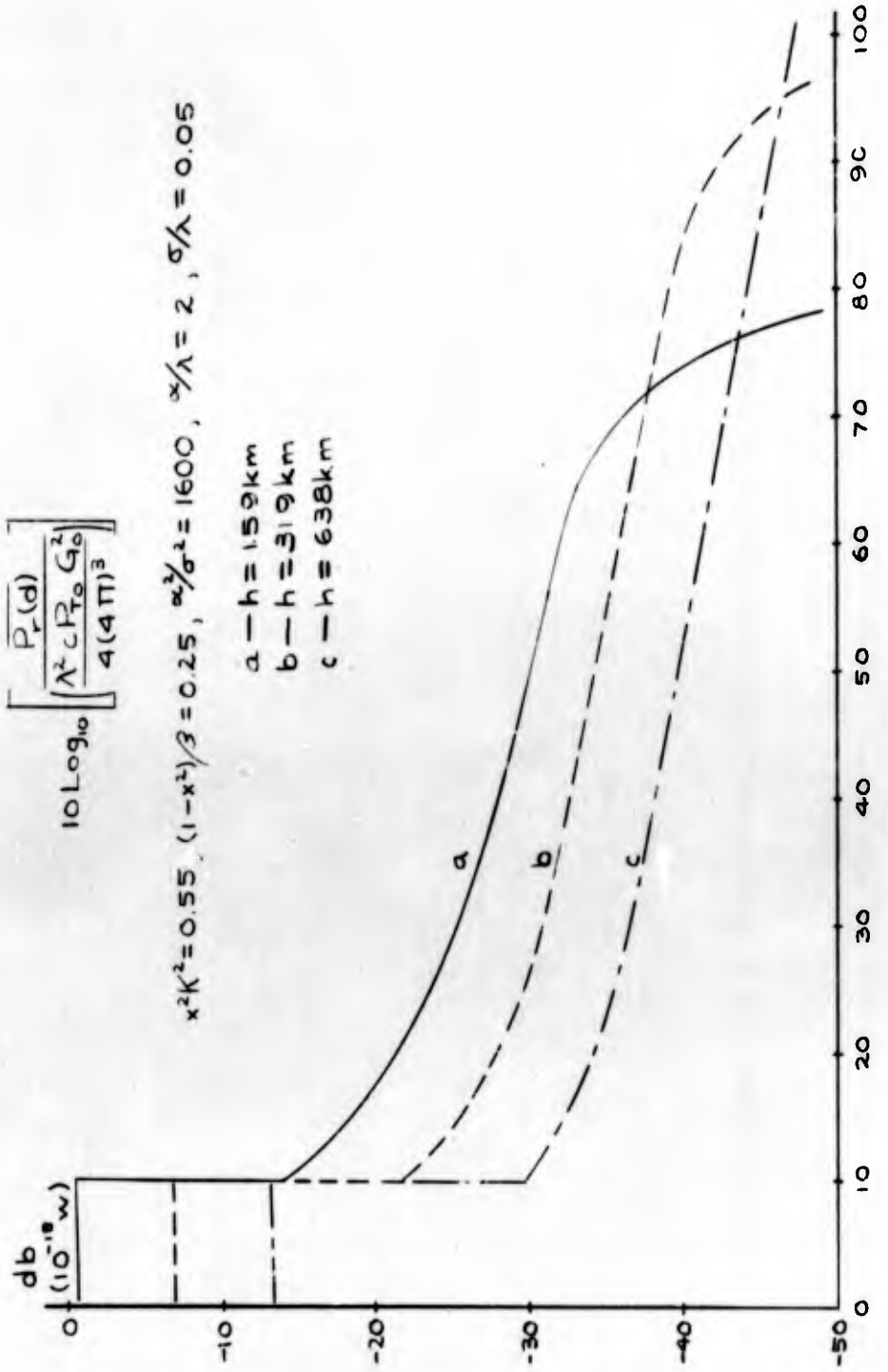
$10\log_{10}\left[\frac{\overline{P_r(d)}}{\frac{\lambda^2 c P_{T_0} G_0^2}{4(4\pi)^3}}\right]$
$x^2K^2=0.55$, $(1-x^2)/\beta=0.25$, $\alpha^2/\sigma^2=1600$, $\alpha/\lambda=2$, $\sigma/\lambda=0.05$
a — h = 159km
b — h = 319km
c — h = 638km
db (10^{-18} w)
0
-10
-20
-30
-40
-50
0
10
20
30
40
50
60
70
80
90
100
Time in μseconds
a
b
c

Figure 7.7

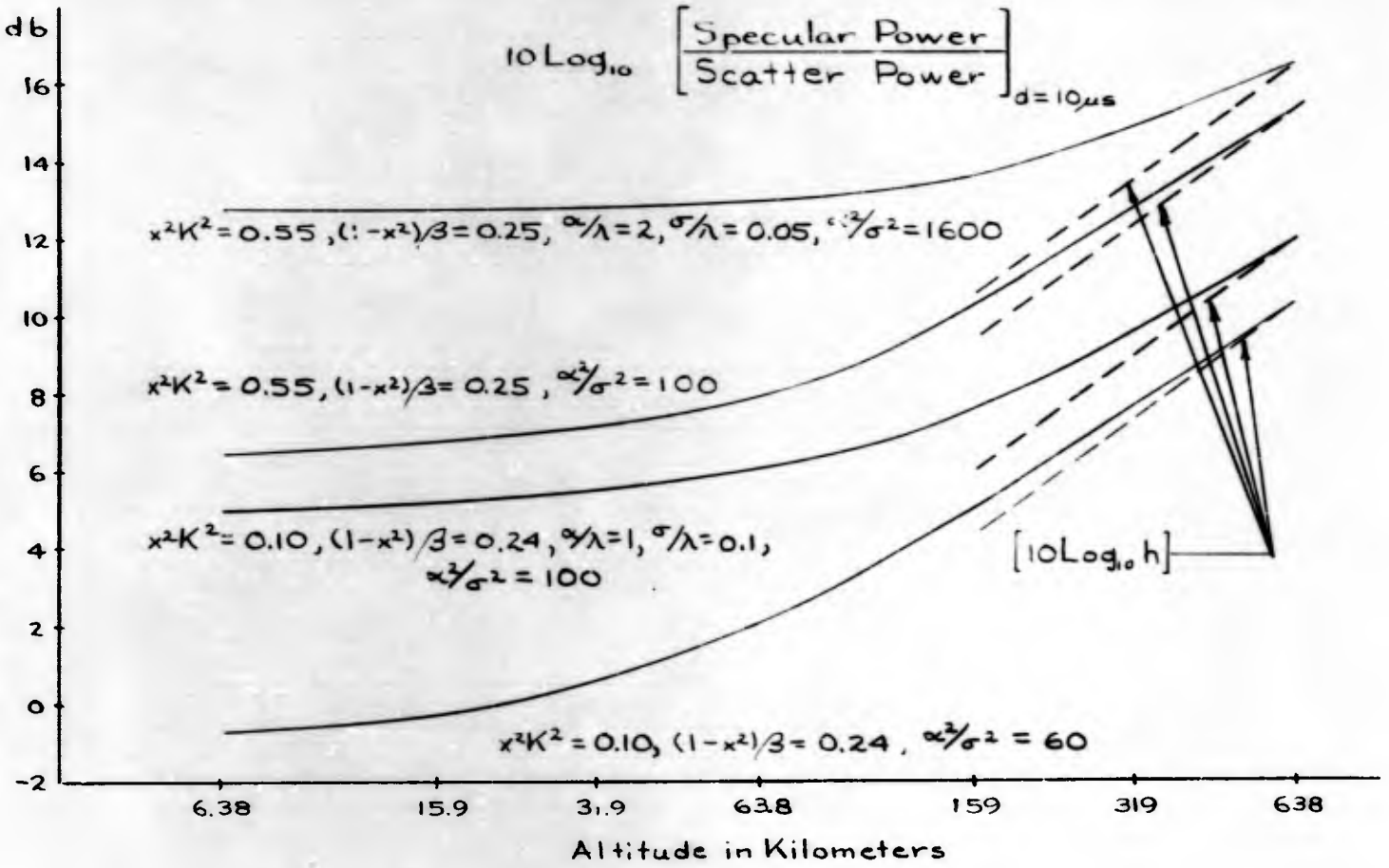
db
16
14
12
10
8
6
4
2
0
-2
$10\,\mathrm{Log}_{10}\left[\frac{\text{Specular Power}}{\text{Scatter Power}}\right]_{d=10\mu s}$
$x^2K^2 = 0.55$, $(1-x^2)/\beta = 0.25$, $\alpha/\lambda = 2$, $\sigma/\lambda = 0.05$, $\alpha^2/\sigma^2 = 1600$
$x^2K^2 = 0.55$, $(1-x^2)/\beta = 0.25$, $\alpha^2/\sigma^2 = 100$
$x^2K^2 = 0.10$, $(1-x^2)/\beta = 0.24$, $\alpha/\lambda = 1$, $\sigma/\lambda = 0.1$,
$\alpha^2/\sigma^2 = 100$
$[10\,\mathrm{Log}_{10}\,h]$
$x^2K^2 = 0.10$, $(1-x^2)/\beta = 0.24$, $\alpha^2/\sigma^2 = 60$
6.38
15.9
31.9
63.8
159
319
638
Altitude in Kilometers

Figure 7.8

The factor x^2 plays an important part in the power return equation as

$$x = e^{-2\left(\frac{2\pi\sigma}{\lambda}\right)^2} \tag{7.10}$$

where σ is the standard deviation of target heights about the mean target surface and λ is the wavelength of radiation.

As an example of the relation that σ has in the separation of specular and scatter, consider the scattering parameters (7.3 iii):

$$x^2K^2 = 0.55, \quad (1-x^2)\beta = 0.25, \quad \alpha^2/\sigma^2 = 100. \tag{7.11}$$

If it is assumed that $K^2 = \beta$ (this has not been proved), then

$$\frac{1-x^2}{x^2} = \frac{0.25}{0.55} = 0.45 , \tag{7.12}$$

$$x^2 = 0.69 , \tag{7.13}$$

$$K^2 = \beta = 0.80 . \tag{7.14}$$

Now

$$x = 0.83 = e^{-2\left(\frac{2\pi\sigma}{\lambda}\right)^2} , \tag{7.15}$$

from which

$$\frac{\sigma^2}{\lambda^2} = 0.0024 . \tag{7.16}$$

At 415 mc,

$$\lambda^2 = 0.52 \text{ meters}. \tag{7.17}$$

Thus,

$$\sigma = 0.067 \text{ meters} , \tag{7.18}$$

$$\alpha = 0.67 \text{ meters} . \tag{7.19}$$

Now assume $\sigma/\lambda = 1$ and $\alpha/\sigma = 10$; this is the same scattering cross-section, $\sigma_o(\theta_i)$, but a different value of x^2.

$$x = e^{-2(2\pi)^2} = e^{-78.9} = 10^{-34.3} . \tag{7.20}$$

Thus, x may be safely assumed to be zero. Then from the previous results

$$(1-x^2)\beta = (1-0)\ (0.80) = 0.80. \tag{7.21}$$

The increase in scatter power is

$$10 \log_{10} \frac{0.80}{0.25} = 5.05 \text{ db} . \tag{7.22}$$

To recapitulate, the ratio σ/λ was increased by a factor of 20.6 which resulted in the complete disappearance of specular power and a 5 db increase in scatter power. To emphasize the dependence of x on σ/λ, x may be written as

$$x = 10^{-34.3(\sigma^2/\lambda^2)} \tag{7.23}$$

Thus, the ratio of σ/λ does not have to be very large to cause the complete disappearance of x.

CHAPTER VIII

CONCLUSIONS

A scalar theory has been presented to explain radar terrain return signals at near-vertical incidence. The method of resolving the return signal into random and specular components is admittedly a first order approximation. However, the results demonstrate that the specular component is always present to some degree and assists in explaining why some experimental phenomena are not explainable by assuming random scatter or specular reflections alone. In Chapter II it was shown that for a normal distribution of heights from mean surface level, the contribution of the specular component varied directly in proportion to the negative exponential of the square of the surface standard deviation expressed in wavelengths. For a very rought surface the signal is nearly all scattered; for a very smooth surface it is nearly all reflected. The relative frequency of occurrence of surfaces which give a measurable amount of specular plus scatter return signal is a matter for further study; most probably an extensive experimental study.

The separation of specular and scatter components of the return field is dependent upon the assumption of a height probability density function. For the purpose of this paper a Gaussian or normal density function was assumed. It is not suggested that the normal density function is the only applicable probability function which can be applied to targets on the earth; however, it seems to be the most

logical to assume. Other density functions may apply to certain classes of targets. For example, water and city targets have a certain degree of periodicity in their surfaces; such surfaces may have probability density functions which are more nearly uniform than normal.

The initial development of the theory was carried out on the assumption of a perfectly conducting surface. If the horizontal scale of surface irregularities is large compared to a wavelength, the Fresnel reflection coefficient may be used to show the approximate reduction in signal due to imperfect conductivity of the surface. A comparable theory is not available for the case where the horizontal scale of irregularities is small compared to wavelength.

An approximate scattering cross-section, as a function of angle of incidence, was obtained on the assumption of a normal bivariate probability density function and a Gaussian correlation function. Here again, these may not be the only probability functions which are applicable to earth targets. If a different density function and/or correlation function is chosen, the analytic form of the scattering cross-section may be quite different.[19]

---

[19] Hayre, H. S., and Moore, R. K., op. cit.

Any effect of depolarization by the rough surface has been lost in the scalar solution of the problem. Compensation for depolarization was included in the form of a constant multiplier of the scatter power integral; however, the depolarization effects may be more significant than this. Katzin, Wolf and Katzin have recently studied depolarization effects in the form of a scattering matrix.[20]

The prediction of high altidude radar terrain return signals by extrapolation of low altitude experimental data is considered to be unsound practice. There are very few earth targets on large land masses which will contain the same statistical information at altitudes of 10,000 feet and 100,000 feet. This is primarily a result of irradiating different target areas at the different altitudes which may cause the analytic form of the scattering cross-section to change. A secondary effect may be analogous to the optical resolution phenomena; large scale irregularities such as mountains, hills, and valleys may be predominate at high altitudes while the small scale irregularities such as grass, trees, and other natural ground cover may be indistinguishable.

---

[20] Katzin, M., Wolf, E. A., and Katzin, J. C., "Investigation of Ground Clutter and Ground Scattering," Final Report, No. CRC-5198-4, Contract AF 19(604)-5198, Electomagnetic Research Corp., Washington, D. C., March 1960.

BIBLIOGRAPHY

1. Chernov, L. A. "Wave Propagation in a Random Medium," McGraw-Hill Book Co., 1960, Chapter 1.

2. Cooper, J. A., "Comparison of Observed and Calculated Near-Vertical Radar Ground Return Intensities and Fading Spectra," Tech. Report EE-10, University of New Mexico Engineering Experiment Station, May 1958.

3. Davies, H., "Reflection of Electromagnetic Waves from a Rough Surface," Proc. Instn. Elect. Engrs., (London), Part IV, Vol. 101, pp. 209-14, August 1954, IEE Monograph No. 90.

4. Edison, A. R., Moore, R. K., and Warner, B. D., "Radar Terrain Return Measured at Near-Vertical Incidence," Trans. I.R.E. P.G.A.P., Vol. AP-8, No. 3, May 1960, pp. 246-54.

5. Edison, A. R., "Radar Terrain Return Statistics at Near-Vertical Incidence," Tech. Report EE-35, Univ. of New Mexico Engineering Experiment Station, Oct. 1960.

6. Fock, V. A., "Generalization of the Reflection Formulas to the Case of Reflection of an Arbitrary Wave from a Surface of Arbitrary Form," Zh. eksp teon. Fiz., Vol. 20, pp. 961-72, 1950.

7. Hayre, H. S., and Moore, R. K., "Theoretical Scattering Coefficient for Near-Vertical Incidence from Contour Maps," J. Res. Nat. Bur. Stand., Vol. 65D., to be published Sept. 1961.

8. Katzin, M., Wolf, E. A., and Katzin, J. C., "Investigation of Ground Clutter and Ground Scattering," Final Report No. CRC-5198-4, AF 19(604)-5198, Electromagnetic Research Corp., Washington, D. C., March 1960.

9. Moore, R. K., and Williams, C. S., Jr., "Radar Terrain Return at Near-Vertical Incidence," Proc. I.R.E., Vol. 45, p. 228, 1957.

10. Moore, R. K., "Resolution of Vertical Incidence Radar Return into Random and Specular Components," Tech. Report EE-6, University of New Mexico Engineering Experiment Station, July 1957.

11. Nelson, D., Hagn, G., Rorden, L., and Clark, N., "An Investigation of the Backscatter of High-Frequency Radio Waves from Land, Sea Water, and Ice," Final Report, Contract Nonr 2917 (00), Stanford Research Institute, May 1960.

Bibliography Part B*

Basore, B. L., and Fursa, A., "Function Heights of Proximity Fuzes," S. C. Tech. Memo 70-55(54), March 1955, (secret)

Bidwell, C. H., "Application of Terrain Return to the Design of Fuzing Radars," S. C. Tech. Memo 219-57(14), Sept. 1957. (secret)

Cooper, J. A., "Comparison of Observed and Calculated Near-Vertical Radar Ground Return Intensities and Fading Spectra," Tech. Report EE-10, Univ. of New Mexico Eng. Exp. Station, May 1958.

Dike, S. H., "Radar Pulse Returns from Extended Targets," Sandia Corp. Tech. Memo SC-2647, 1953.

Edison A. R., "Reflection and Scattering Coefficients from several Types of Terrains," Tech. Report EE-8, Univ. of New Mexico Eng. Exp. Station, Sept., 1957.

Edison, A. R., Janza, F. J., Moore, R. K., and Warner, B. D., "Radar Cross Sections of Terrain Near-Vertical Incidence at 415 Mc," Tech. Report EE-15, Univ. of New Mexico Eng. Exp. Station, 1958.

Glascock, R. B., "Design of an Experiment to Separate Specular and Scattered Radar Return," Tech. Report EE-9, Univ. of New Mexico Eng. Exp. Station, May 1958.

Gragg, D. M., "A Method for Ascertaining the Effect of Large Targets Present in Terrain Return Signals," S. C. Tech. Memo 187-54(54), September 1954.

Gragg, D. M., and Tiede, K. F., "Probability Distribution of Two Sinusoids in Noise," Sandia Corp. Tech. Memo. 94-53-54, August 1954.

Gragg, D. M., Hessemer, R. A., and Moore, R. K., "Survey of Terrain Return Data," S. C. Tech. Memo. 194-55(54), Sept., 1955. (confidential)

Hessemer, R. A., Jr., and Williams, C. S., Jr., "Determination of Radar Cross Section for a Scattering Ground." Sandia Corp. Tech. Memo 206-54-54, Sept., 1954.

Hessemer, R. A., Jr., and Williams, C. S., Jr., "Solution of the Integral Equation which Determines Radar Cross Section For a Scattering Ground," Sandia Corp. Tech. Memo 207-54-54, Sept. 1954.

---

* Many of the papers listed in this section have not been distributed.

Hessemer, R. A., Jr., and Gragg, D. M., "Signal Strengh Vs. Altitude for Vertical Incidence Radar," S. C. Tech. Memo 40-55-54.

Hessemer, R. A., Jr., "The Sampling Problem in Low Frequency Radar Terrain Return," Sandia Corp. Tech. Memo 193-54-54, Sept., 1954.

Janza, F. J., Moore, R. K., Warner, B. D., "Radar Cross Sections of Terrain Near Vertical Incidence at 415 Mc, 3800 Mc and Extension of Analysis to X-Band," Tech. Report EE-21, Univ. of New Mex. Engr. Exp. Sta., May 1959.

Janza, F. J., and Hessemer, R. A., and Williams, C. S., Jr., "Pulse Response of Terrain Return Program Receivers," S. C. Tech. Memo 208-54-54, Sept. 1954.

Moore, R. K., "Effect of Precipitation on the Design of Radio Altimeters," Sandia Corp. Tech. Memo SC-3811 (TR), April, 1956.

Moore, R. K., "Normal Incident Reflection of Dipole Radiation from a Plane Interface," Sandia Corp. Tech. Memo 199-56-44, Sept., 1956.

Moore, R.K., "Radar Terrain Return," S. C. Tech. Memo 20-52-15, 1952. (confidential)

Moore, R. K., and Gragg, D. M., "Preliminary Results of Terrain Return Program," S. C. Tech. Memo 5-54-54. (secret)

Moore, R. K., "Resolution of Vertical Incidence Radar Return into Random and Specular Components," Tech. Report EE-6, Univ. of New Mexico Eng. Exp. Station, July 1957.

Usry, J. M., and Glascock, R. B., "Converting Measured Antenna Patterns to Spherical Coordinates," Tech. Report EE-3, Univ. of New Mexico Exp. Stat., March 1957.

Welch, P. D., "A Method for Obtaining the Variance of Averages over Non-Independent Samples from a Stationary Time Series," New Mexico College of A and MA, Physical Science Lab. Report AER 11-W, December 1955.

Welch, P. D., "Progress Report on Interpretation and Prediction of Radar Terrain Return Fading Spectra," New Mexico College of A and MA, Phys. Sci. Lab. Reports AER 14-W, May 1955, May 1955, AER 18-A, February 1956, AER 18-B, May 1956.

Welch, P. D., "The Covariance Spectrum of Two Points on a Radar Terrain Return Pulse," New Mexico College of A and MA, Phys. Sc. Lab. Report AER 20-B, July, 1956.

Williams, C. S., Jr., "Reference Charts Concerning Mean Radar Terrain Return," S.C. Tech. Memo 223-55(54), December, 1955.

Williams, C. S., Jr., "A Computor to Solve one Form of Volterra's Integral Equation," S. C. Tech. Memo 104-55-54, 1955.

Williams, C. S., Jr., "A Proposal for Two Computers Dealing with the Convolution Integral," M. S. Thesis, Univ. of New Mexico 1955.

Williams, C. S., Jr., Bidwell, C. H., and Gragg, D. M., "Radar Return from the Vertical for Ground and Water Surfaces," Sandia Corp. Monograph SCR-107, April 1960.

"A Symposium on Terrain Return," S. C. Tech. Memo 3522 (TR), 1955. (confidential)

"Supplement, A Symposium on Terrain Return," S. C. Tech. Memo 3642 (TR), 1955. (secret)

"A Symposium on Radar Return," U. S. Naval Ordnance Test Station, China Lake, Calif., and the Univ. of New Mex. Engr. Exp. Stat., May 1959.

"Bimonthly Progress Report on Terrain Reflection Studies," New Mexico College of A and MA, Phys. Sci. Lab. Report AER-2, May 1952.

"Reduction and Analysis of Radar Terrain Return Data," New Mex. College of A and MA, Phys. Sci. Lab. Report AER-4.

APPENDIX A

BOUNDARY CONDITIONS FOR FOCK'S DEVELOPMENT OF AN ARBITRARY WAVE REFLECTED FROM AN ARBITRARY SURFACE

Let the field of an incident wave be represented by

$$\underline{E}^{o}e^{jk_1\varphi} \quad , \quad \underline{H}^{o}e^{jk_1\varphi} \quad , \tag{A.1}$$

where E^{o} and H^{o} denotes amplitude, and φ is the phase expressed in units of length, and

$$|\nabla \varphi|^2 = 1 \tag{A.2}$$

The amplitudes E^{o} and H^{o} would be constant if the incident field was a plane wave; however, in that which follows the components of the vectors $\underline{E}^{o}$ and $\underline{H}^{o}$ shall be considered as slowly varying functions of space coordinates. $\underline{E}^{o}$ and $\underline{H}^{o}$ are also taken as the values of the incident field on the surface of the reflecting body. The corresponding values of the reflected field at the surface of the reflecting body will be designated by $\underline{E}'$ and $\underline{H}'$.

Let $\underline{u}$ be a unit vector in the direction of propagation of the incident wave, $\underline{u}'$ be a unit vector in the direction of propagation of the reflected wave, and $\underline{n}$ be a unit normal to the surface of the body at the point of reflection. Then by the law of reflection the unit vectors $\underline{u}$, $\underline{u}'$, and $\underline{n}$ are related by

$$\underline{u}' = \underline{u} - 2\underline{n}(\underline{u}\cdot\underline{n}) \quad . \tag{A.3}$$

Furthermore

$$\underline{u}' \cdot \underline{n} = -\underline{u} \cdot \underline{n} = \cos \theta, \tag{A.4}$$

where θ is the angle of incidence. The values $\underline{u}$ and $\underline{u}'$ are proportional to the gradient and phase of the incident and reflected wave respectively.

If the variations in amplitude of E^c and H^c over one wavelength are neglected, the following results are obtained from Maxwell's equations:

$$\underline{u} \times \underline{E}^o = \eta_1 \underline{H}^o \quad , \quad \underline{u} \cdot \underline{E}^c = 0, \tag{A.5}$$

$$\underline{u} \times \underline{H}^o = -\frac{\underline{E}^c}{\eta_1} \quad , \quad \underline{u} \cdot \underline{H}^o = 0, \tag{A.6}$$

and analogously for the reflected wave

$$\underline{u}' \times \underline{E}' = \eta_1 \underline{H}' \quad , \quad \underline{u}' \cdot \underline{H}^c = 0, \tag{A.7}$$

$$\underline{u}' \times \underline{H}' = -\frac{\underline{E}'}{\eta_1} \quad , \quad \underline{u}' \cdot \underline{H}' = 0, \tag{A.8}$$

where η_1 is the intrinsic impedance of medium 1, the medium containing the source of energy.

Let μ_1 and μ_2 be the magnetic permeability of medium 1 and medium 2 respectively, and k_1 and k_2 be the wave numbers in medium 1 and medium 2 respectively. Here medium 2 is understood to be the reflecting body. The Fresnel reflection coefficients are

$$N = \frac{\mu_1 k_2^2 \cos\theta - \mu_2 k_1 \sqrt{k_2^2 - k_1^2 \sin^2\theta}}{\mu_1 k_2^2 \cos\theta + \mu_2 k_1 \sqrt{k_2^2 - k_1^2 \sin^2\theta}} \quad , \tag{A.9}$$

$$M = \frac{\mu_2 k_1 \cos\theta - \mu_1 \sqrt{k_2^2 - k_1^2 \sin^2\theta}}{\mu_2 k_1 \cos\theta + \mu_1 \sqrt{k_2^2 - k_1^2 \sin^2\theta}} \tag{A.10}$$

For polarization normal to the plane of incidence

$$\text{(i)} \quad N = \frac{H'}{H^\circ} ,$$

$$\text{(ii)} \quad N = \frac{n \cdot E'}{n \cdot E^\circ} , \tag{A.11}$$

or

$$\text{(iii)} \quad N = - \frac{n \times E'}{n \times E^\circ} .$$

For polarization parallel to the plane of incidence

$$\text{(i)} \quad M = \frac{E'}{E^\circ} ,$$

$$\text{(ii)} \quad M = \frac{n \cdot H'}{n \cdot H^\circ} , \tag{A.12}$$

or

$$\text{(iii)} \quad M = \frac{n \times H'}{n \times H^\circ} .$$

Choosing case (ii) from both of the above sets of relations, the reflected wave in terms of the incident wave and the Fresnel reflection coefficients is

$$n \cdot E' = N (n \cdot E^\circ) , \tag{A.13}$$

$$n \cdot H' = M (n \cdot H^\circ) . \tag{A.14}$$

The transmitted wave is of no interest here and its corresponding equations are omitted.

Equations (A.7), (A.13) , and (A.14) can be solved for the vectors $\underline{E}'$ and $\underline{H}'$ in terms of $\underline{E}^o$ and $\underline{H}^o$. Let

$$\underline{n}\cdot\underline{E}^o = E_n^o \quad , \quad \underline{n}\cdot\underline{H}^o = H_n^o \quad . \tag{A.15}$$

Utilizing the expression

$$\underline{u}' = \underline{u} - 2(\underline{u}\cdot\underline{n})\underline{u} \tag{A.16}$$

it is found that

$$\underline{E}' \sin^2\theta = NE_n^o\,(\underline{n}\cos 2\theta + \underline{u}\cos\theta) + M\,H_n^o\,(\underline{n}\times\underline{u}) \tag{A.17}$$

$$\underline{H}' \sin^2\theta = MH_n^o\,(\underline{n}\cos 2\theta + \underline{u}\cos\theta) - N\,E_n^o\,(\underline{n}\times\underline{u}) \tag{A.18}$$

These are the values of the reflected wave at the surface of the reflecting body as derived from the Fresnel reflection formulas.

APPENDIX B

AN APPROXIMATE SCATTERING CROSS-SECTION OF A ROUGH PLANE

In this section an approximate scattering cross-section for a rough plane is developed; the result is suitable for use with Equation (5.5).

Here again it is assumed that the Huygen's-Kirchhoff integral can be applied and the return power is

$$P_r = \mathrm{Re}\,\frac{A_r}{8\pi\lambda^2}\iint_{A\,A'}\frac{P_T\cos\theta_i\cos\theta_i'}{R^2R'^2}\,e^{-j2k(R-R')}\,dA\,dA' \qquad (B.1)$$

by the same reasoning as in Chapter VI.

The geometry to be considered is that of a spherical wave scattered from a rough plane; this is shown in Figures B.1, B.2, B.3 and B.4.

From Figure B.1, the actual radar range, R_n in terms of the mean range, R_{on}, and the deviation of the scatterers, δ_n, about the mean plane, is

$$R_n^2 = R_{on}^2 + \delta_n^2 - 2\,\delta_n R_{on}\cos\theta_i. \qquad (B.2)$$

By a development identical to that in Chapter II,

$$R_n \approx R_{on} - \delta_n\cos\theta_i. \qquad (B.3)$$

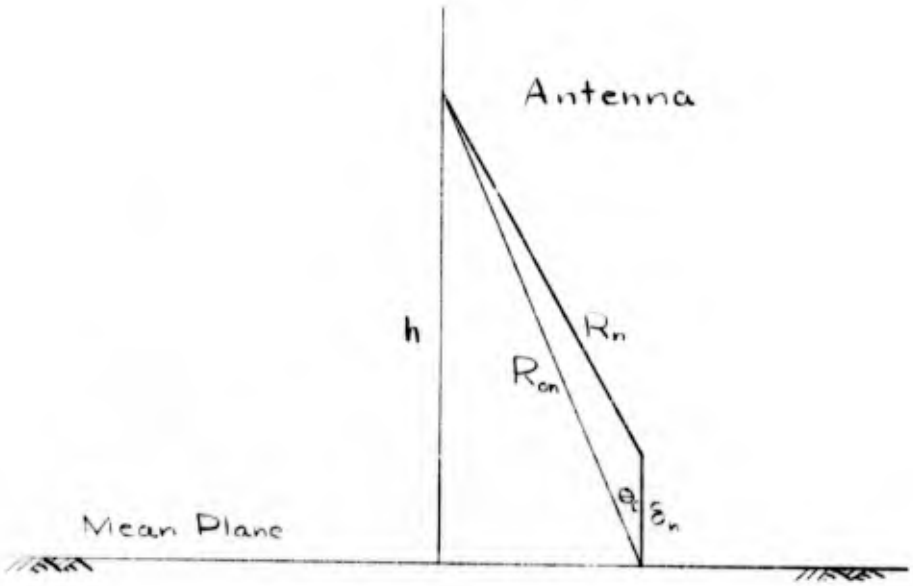

Figure B.1

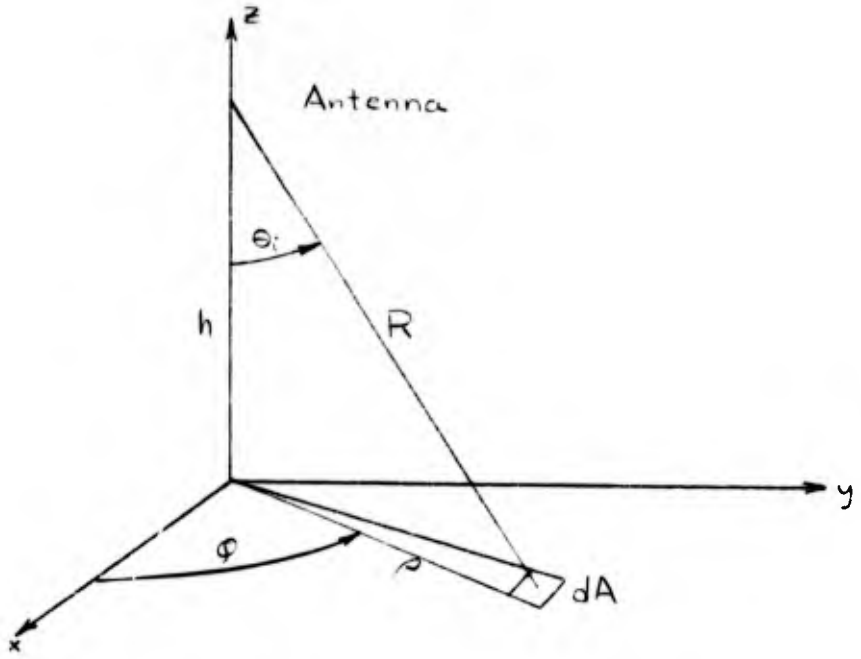

Figure B.2

Thus, in general

$$R \approx R_o - \delta \cos\theta_i \tag{B.4}$$

and

$$R' \approx R_o' - \delta' \cos\theta_i' \ . \tag{B.5}$$

An area element is shown in Figure B.2 from which

$$dA = \rho \, d\rho \, d\varphi \ . \tag{B.6}$$

But

$$R^2 = h^2 + \rho^2 , \tag{B.7}$$

and

$$RdR = \rho \, d\rho \ . \tag{B.8}$$

Likewise

$$R'dR' = \rho' d\rho' \ . \tag{B.9}$$

Because of the assumed statistical dependence of R and R', new coordinates and variables of integration are defined in Figure B.3. Associating the primed quantities with the unprimed quantities through the new variables s and ζ ,

$$R' = R+s \tag{B.10}$$

$$\varphi' = \varphi+\zeta \tag{B.11}$$

where s and ζ represent, respectively, the change in range and change in azimuth in moving from A to B. Hence,

$$dR' = ds \tag{B.12}$$

$$d\varphi' = d\zeta \tag{B.13}$$

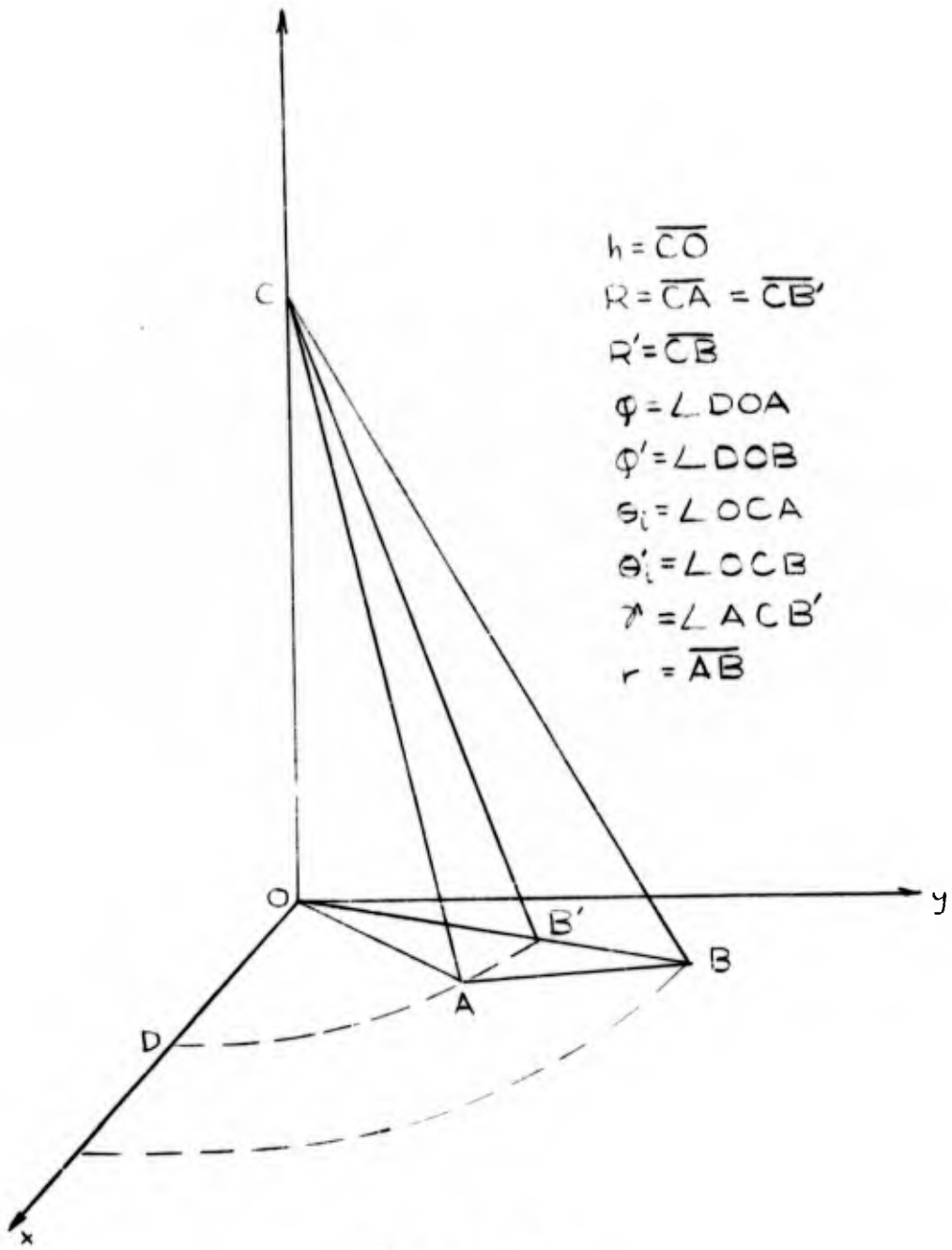
h = $\overline{CO}$
R = $\overline{CA}$ = $\overline{CB'}$
R' = $\overline{CB}$
φ = ∠ DOA
φ' = ∠ DOB
θ = ∠ OCA
θ' = ∠ OCB
γ = ∠ ACB'
r = $\overline{AB}$
C
O
B'
B
A
D
y
x

Figure B.3

With these results, the expression for the received power is

$$P_r = \frac{A_r}{8\pi\lambda^2} \iiint_A \iiint_{A'} \frac{P_T \cos\theta_i \cos\theta_i' \, e^{-j2k(s - \delta\cos\theta_i + \delta'\cos\theta_i')}}{R R'} \, dR\, d\varphi\, ds\, d\zeta \, . \tag{B.14}$$

Note that the only difference between this equation and Equation (6.20) is the absence of the multiplicative constant a^2/b^2.

Once again assuming the normal bivariate probability density function, $p(\delta, \delta')$, (Equation (6.22)), the mean value of

$$f(\delta, \delta') = e^{-j2k(\delta'\cos\theta_i' - \delta\cos\theta_i)} \tag{B.15}$$

is

$$\overline{f(\delta, \delta')} = e^{-2k^2\sigma^2(\cos^2\theta_i - 2\rho\cos\theta_i\cos\theta_i' + \cos^2\theta_i')} \, . \tag{B.16}$$

from Equations (6.23) through (6.28) .

By the same reasoning as given in Chapter VI, the correlation coefficient, ρ, is assumed to be

$$\rho = e^{-r^2/\alpha^2} \approx 1 - r^2/\alpha^2 \, . \tag{B.17}$$

Here again, Davies' approximation for the distance r is applied;

$$r^2 \approx R^2 \gamma^2 + s^2 \csc^2\theta_i' \, . \tag{B.18}$$

From spherical trigonometry,

$$\cos \gamma = \cos^2\theta_i + \sin^2\theta_i \cos \zeta \quad ; \tag{B.19}$$

and approximating $\cos \gamma$ with

$$1 - \frac{\gamma^2}{2} \approx \cos\gamma = \cos^2\theta_i + \sin^2\theta \cos \zeta \, , \tag{B.20}$$

$$\gamma^2 \approx 2 - 2\cos^2\theta_i - 2\sin^2\theta_i \cos \zeta \, . \tag{B.21}$$

Then

$$\rho \approx 1 - \frac{2R^2}{\alpha^2}\sin^2\theta_i + \frac{2R^2}{\alpha^2}\sin^2\theta_i \cos\zeta - \frac{s^2}{x^2}\csc^2\theta_i' \, . \tag{B.22}$$

The power return integral now has the form

$$P_r = \frac{1}{32\pi^2} \iiint_{A}\iint_{A'} \frac{P_T}{RR'} \cos\theta_i \cos\theta_i' \exp\Bigg\{ -j2ks$$

$$- 2k^2\sigma^2\Bigg[\cos^2\theta_i + \cos^2\theta_i' + 2\cos\theta_i\cos\theta_i'\Bigg(-1 + \frac{2R^2}{\alpha^2}\sin^2\theta_i$$

$$- \frac{2R^2}{\alpha^2}\sin^2\theta_i\cos\zeta + \frac{s^2}{\alpha^2}\csc^2\theta_i'\Bigg)\Bigg]\Bigg\} \, dR\, d\phi\, ds\, d\zeta \tag{B.23}$$

Moore and Williams integral in the plane has the form

$$P_r = \frac{\lambda^2}{(4\pi)^3}\iint_A \frac{P_T\,\sigma_o(\theta_i)}{R^3}\, dR\, d\phi = \frac{\lambda^2}{32\pi^2}\int \frac{P_T\,\sigma_o(\theta_i)\, dR}{R^3} \tag{B.24}$$

where an isotropic antenna has been assumed. Comparing these two expressions for the power return, it must be that

$$\sigma_o(\theta_i) = \mathcal{R}e\ \frac{R^2\cos\theta_i}{\lambda^2}\iiint\frac{\cos\theta_i'}{R'}\exp\left\{-j2ks\right.$$

$$-2k^2\sigma^2\left[\cos^2\theta_i+\cos^2\theta_i'+2\cos\theta_i\cos\theta_i'\left(-1+\frac{2R^2}{\alpha^2}\sin^2\theta_i\right.\right.$$

$$\left.\left.\left.-\frac{2R^2}{\alpha^2}\sin^2\theta_i\cos\zeta+\frac{s^2}{\alpha^2}\csc^2\theta_i'\right)\right]\right\}d\varphi\,ds\,d\zeta\,. \qquad \text{(B.25)}$$

The limits of integration are

$$\begin{aligned} -\pi &\le \varphi \le \pi \\ -\pi &\le \zeta \le \pi \\ -(R-h) &\le s \le (R_o-R) \end{aligned} \qquad \text{(B.26)}$$

where R_o is the maximum range within the irradiated area. This integral, and its limits, is the same form as Equation (6.51) and its limits; hence, if the same approximations are made in the evaluation, the results will be identical.

$$\sigma_o(\theta_i) = \frac{\alpha^2}{8\sigma^2}\ e^{-\frac{\alpha^2}{4\sigma^2}\tan^2\theta_i}\ ,\ \frac{2k^2\sigma^2R^2}{\alpha^2}\sin^2 2\theta_i \ge 2 \qquad \text{(B.27)}$$

To prove that this result is valid for $\theta_i = 0^\circ$, a slightly different argument from that in Chapter VI is presented. Evaluating the integral form of $\sigma_o(\theta_i)$ at $\theta_i = 0^\circ$ as a function of r,

$$\sigma_o(0^\circ) \approx \frac{h}{\lambda^2}\int_{-\pi}^{\pi}\int_{-\pi}^{\pi}\int_{0}^{R_o-h} e^{-j2ks - \frac{4k^2\sigma^2 r^2}{\alpha^2}}\, ds\, d\xi\, d\varphi \qquad \text{(B.28)}$$

From Figure B.4

$$r^2 = 2hs + s^2 \qquad \text{(B.29)}$$

As it has been shown that integrals of this form converge rapidly for small values of r^2, then a good approximation is

$$r^2 \approx 2hs \quad \text{for} \quad 2hs > s^2 \,. \qquad \text{(B.30)}$$

Hence

$$\sigma_o(0^\circ) \approx \frac{(2\pi)^2 h}{\lambda^2}\int_0^\infty (\cos 2ks)\, e^{-\frac{8k^2\sigma^2 h}{\alpha^2}s}\, ds \qquad \text{(B.31)}$$

where the upper limit has been extended to infinity. This evaluates to

$$\sigma_o(0^\circ) \approx \frac{(2\pi)^2 h}{\lambda^2}\,\frac{\frac{8k^2\sigma^2 h}{\alpha^2}}{\left[\frac{8k^2\sigma^2 h}{\alpha^2}\right]^2 + 4k^2} \qquad \text{(B.32)}$$

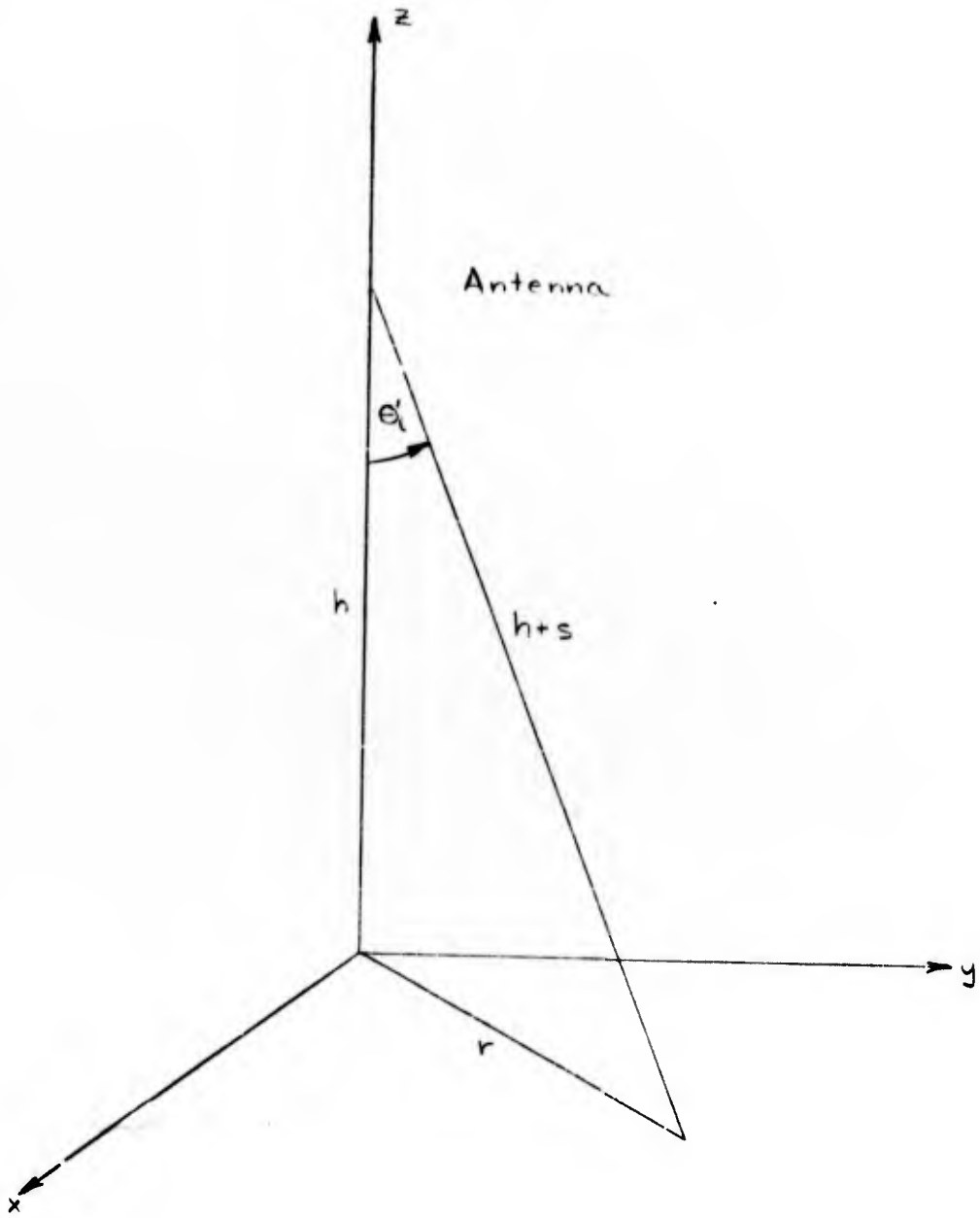

Figure B.4

Rearranging,

$$\sigma_o(0^\circ) \approx \frac{2(2\pi)^2 h^2 \sigma^2}{\lambda^2 \alpha^2} \frac{1}{\left[\frac{4k\sigma^2 h}{\alpha^2}\right]^2 + 1} \tag{B.33}$$

If

$$\left[\frac{4k\sigma^2 h}{\alpha^2}\right]^2 >> 1 \tag{B.34}$$

then

$$\sigma_o(0^\circ) \approx \frac{\alpha^2}{8\sigma^2} \tag{B.35}$$

Thus,

$$\sigma_o(\theta_i) \approx \frac{\alpha^2}{8\sigma^2} e^{-\frac{\alpha^2}{4\sigma^2}\tan^2\theta_i}, \quad \frac{2k^2\sigma^2 R^2}{\alpha^2}\sin^2\theta_i \geq 0 \tag{B.36}$$

This is the same form as the result in Chapter VI.

APPENDIX C

Experimentally Determined Scattering Parameters

If the results of the preceding sections are to be useful to the system designer, some typical values of the terrain scattering parameters, x^2K^2, $(1-x^2)\beta$, and α^2/σ^2, are required. The numerical values of these parameters, which are presented in Table CI , were obtained from the results of an extensive radar terrain return experiment carried out by the Sandia Corporation, Albuquerque, New Mexico, during the years 1952 to 1955.

The experimental data was obtained by flying a C-47 aircraft, equipped with 415 and 3800 mc radar, over selected target areas in the United States. The results presented in Table CI were obtained at altitudes of 4000, 7000, and 12000 feet. These targets were deliberately selected to eliminate large scale roughness, such as hills, mountains, and valleys, and selected for homogeneity of small scale roughness such as trees, buildings, flat desert, etc. Extrapolation of these results to much higher altitudes seems to indicate that the specular component of the return will predominate as the scatter component falls off with the inverse cube of the altitude, versus the inverse square variation for the specular component. If this altitude relationship between specular and scatter components does occur it will probably be found over the open sea. However, this should not be expected over

large land masses as any appreciable increase in altitude will add a large area to the irradiated region; homogeneity of large land areas is not a feature of the earth's surface.

Table CI

EXPERIMENTALLY DETERMINED SCATTERING PARAMETERS AND THEIR TARGET DESCRIPTIONS

$$\sigma_o(\theta_i) \approx \frac{\alpha^2}{8\sigma^2} e^{-\frac{\alpha^2}{4\sigma^2}\tan^2\theta_i}$$

Forest, Pine Island, Minnesota. The target area was very flat and densely covered with pine, hemlock, birch, white ash, and elm trees from 20 to 40 feet in height.

Freq. in mc.	x^2K^2	$(1-x^2)\beta$	α^2/σ^2	Range of fading
415	0	0.13	34	14.7 db
3800	0	0.45	16	15.9 db

Forest, Presque Isle, Maine. The target had a snow-and-ice-covered rolling surface with a homogeneous covering of snow-bare evergreen fir and pine trees from 20 to 50 feet in height.

Freq. in mc	x^2K^2	$(1-x^2)\beta$	α^2/σ^2	Range of fading
415	0	0.87	34	14.7 db
3800	0	0.88	22	17.5 db

Snow-Covered Farmland, Wahpeton, North Dakota. The target area was flat crop land with two dry stream beds and an eight inch covering of dry snow.

Freq. in mc.	x^2K^2	$(1-x^2)\beta$	α^2/σ^2	Range of fading
415	0.066	0.24	53	14.2 db
3800	0.063	0.85	57	15.8 db

Farmland, Cameron, Missouri. The target area was flat pasture and crop land with a single line railroad.

Freq. in mc.	x^2K^2	$(1-x^2)\beta$	α^2/σ^2	Range of fading
415	0.092	0.24	60	18.7 db
3800	0.34	1.98	70	14.1 db

Farmland, Sioux City, Iowa. The target area was flat crop land which had recently been plowed.

Freq. in mc.	x^2K^2	$(1-x^2)\beta$	α^2/σ^2	Range of fading
415	0.049	0.22	70	16.3 db
3800	0.090	0.26	52	14.6 db

Industrial Area, Minneapolis, Minnesota. The target contained a predominant number of metal roofed factory buildings with a railroad yard at one edge.

Freq. in mc.	x^2K^2	$(1-x^2)\beta$	α^2/σ^2	Range of fading
415	0	0.28	58	16.6 db
3800	0.23	1.73	42	14.9 db

Residential Area, Minneapolis, Minnesota. The target area was one and two story brick and frame houses with pitched roofs, and had many old, well-established trees.

Freq. in mc.	x^2K^2	$(1-x^2)\beta$	α^2/σ^2	Range of fading
415	0	0.25	59	16.3 db
3800	0.029	0.98	48	14.1 db

Apartment Buildings, Kansas City, Missouri. The majority of the buildings were built of brick, flat roofed, and several stories tall.

Freq. in mc.	x^2K^2	$(1-x^2)\beta$	α^2/σ^2	Range of fading
415	0	0.25	59	17.3 db
3800	0.27	1.63	70	18.5 db

Desert, Salton Sea, California. The target area was flat, arid, sandy, and barren.

Freq. in mc.	x^2K^2	$(1-x^2)\beta$	α^2/σ^2	Range of fading
415	0.0044	0.052	75	16.4 db
3800	0.20	0.29	59	16.4 db

Water, Lake Benidji, Minnesota. The lake surface was moderately rough with ripples and swells about 15 to 20 inches vertically from peak to trough and three to four feet horizontally from peak to peak.

Freq. in mc.	x^2K^2	$(1-x^2)\beta$	α^2/σ^2	Range of fading
415	0	5.05	68	8.2 db
3800	3.11	8.52	95	16.0 db

Water, Salton Sea, California. The air over the target was quite calm at the time of the flights and the lake surface was relatively smooth.

Freq. in mc.	x^2K^2	$(1-x^2)\beta$	α^2/σ^2	Range of fading
415	0.59	1.57	96	16.2 db
3800	0	6.94	228	18.8 db

Note that some of the values reported in Table CI do not agree very well with the results predicted by theory; however, this detracts nothing from the usefulness of these results. The reason for computing these parameters is to remove the radar system constants and altitude from the experimental data. As these parameters were computed from a median pulse, computed pulses will also be median pulses; i.e., at any given delay time within an ensemble of return pulses, one-half the power will be above the corresponding power point on the median return pulse. It is extremely improbable that any individual return pulse from an ensemble of return pulses will have the same shape as the median pulse.

DISTRIBUTION LIST

Department of the Navy
Chief, Bureau of Ordnance
Washington 25, D. C.

Ad3 (1)
Ad6 (3)
ReW (3)
ReW-2 (2)
Rex (1)
Rea (1)
PLe (1)
ReS1-3 (1)
Re02 (1)
ReS4 (1)

Commander
U. S. Naval Ordnance Test Station
China Lake, California
Code 4035 (24)
Code 753 (2)

Director, Naval Ordnance Laboratory, Corona, California (1)
Director, Naval Ordnance Laboratory, White Oak, Silver Spring, Md. (1)
U. S. Navy Electronics Laboratory, San Diego, California (1)
Commander, U. S. Naval Proving Ground, Dahlgren, Va. (1)
Bureau of Aeronautics, The Pentagon
Washington 25, D. C.
Armament Division 1-W46 (1)
Electronics Division 1-W99 (1)
Guided Missile Division 2-W44 (1)

Department of the Army
Office Chief of Ordnance, 2 E 400, The Pentagon (1)
Commanding Officer, Ballistics Research Lab., Aberdeen Proving Ground, Md. (1)
Commanding Officer, Picatinny Arsenal, Dover, N. J. (1)
Director OSWD, Army Field Forces, Ft. Bliss, Texas (1)
Director Guided Missiles Division, 4 E 440, The Pentagon (1)
Director of New Developments and Operational Evaluation Division, 5 D 500, The Pentagon
Chief, Office of Naval Research, 1804 The Pentagon (1)
Diamond Ordnance Fuze Laboratories
Connecticut and Van Ness Sts., N. W.
Washington 25, D. C.
Mr. Clyde Hardin (2)
Mr. Henry Kalmus (1)
Mr. Billy W. Horton (1)
Mr. John W. Seaton (1)
DOFL Library (2)
Lab 40 Library (2)

U. S. Army Signal Engineering Laboratories
Ft. Monmouth, N. J.
Technical Document Center (1)
Commanding General
Redstone Arsenal, U. S. Army
Redstone, Alabama
Technical Library (1)

Department of the Air Force
Air Force Cambridge Research Center
L. G. Hanscom Field, Medrord, Mass.
Electronics Research Directorate (2)
Wright Air Development Center
Wright-Patterson AFB, Ohio
Altimeter Branch (1)
Aircraft Radiation Laboratory (1)
WCSM (1)
WCLGW (1)

Emerson Research Laboratories
701 Lamont Street, N. W.
Washington 10, D. C.
Dr. Reynor Wilson (1)

Officer in Charge
Jet Propulsion Laboratory
4800 Oak Grove Drive
Pasadena 2, California
Mr. Irl E. Newlan, Reports Group (1)
Armed Services Tech. Information Agency
Arlington Hall Station
Arlington 12, Va.
TIPDR (20

Lockheed Aircraft Corporation (1)
Missile Systems Division
P.O. Box 504
Sunnyvale, California

Franklin Institute Lab. for Research & Development
Philadelphia, Pennsylvania
Mr. S. Charp (1)

Bell Telephone Laboratory (1)
Whippany N. J.
Via INSMAT, Newark
Naval Industrial Reserve Shipyard
Building 13
Port Newark, N. J.

Massachusetts Institute of Technology
Research Laboratory of Electronics
Cambridge 39, Mass.
R. L. E. Document Room (2)

Farnsworth Electronics Company
Ft. Wayne, Indiana - Miss Marlene Alt (1)

Radio Corporation of America
Missile and Surface Radar
Moorestown, N. J.
Mrs. A. G. Campbell (1)

Engineering Document Center
Gilfillan Brothers, Inc.
1815 Venice Blvd.
Los Angeles 6, California
Mr. A. J. McClelland (1)

General Electric Company
Missile and Ordnance Systems
8198 Chestnut Street
Philadelphia, Penn.
L. Chasen (1)

Convair
P.O. Box 1950
San Diego 12, California
Mrs. Dora B. Burke (1)
Via Bureau Aeronautics Rep.,
Convair - San Diego, Calif.

Sylvania Electric, Inc.
Wattham Laboratory Library
100 First Avenue
Matham 54, Mas.
Mary Timmers (1)

Air Force, Office of Scientific Research
Washington 25, D. C.
Dr. Wm. J. Offing

Department of the Air Force
Director Project RAND (1)
1700 Main Street
Santa Monica, California

Applied Physics Laboratory
John Hopkins University
8621 Georgia Avenue
Silver Spring, Md.
Mr. Isadore Katz (1)
Reports Office (2)

Bendix Aviation Corporation
Research Laboratory Division
P.O. Box 5115
Detroit, Michigan
Reports Library (1)
Via Inspector of Naval Material
310 East Jefferson Avenue
Detroit 25, Michigan

Eastman Kodak Company (1)
Navy Ordnance Division
Rochester 14, N. Y.

Office of the Secretary of Defense, The Pentagon - Washington, D.C.
Asst. Secretary for Research and Development, 3 E 1074 (1)
Asst. Secretary for Applications Engineering, 3 E 1006 (1)
Director of Guided Missiles, 3 E 1006 (1)
Director Ord. and Transportation Equipment, 3 D 1027 (1)
Panel on Atomic Energy, 3 E 1085 (1)
Committee on Guided Missiles, 3 E 130 (1)
Panel on Ordnance, 3 D 1083 (1)
Armed Forces Special Weapons Project, 1 B 670 (1)
Commanding General FC/AFSWP, Sandia Base, N. M. (1)

University of Michigan
Willow Run Research Center
Ypsilanti, Michigan
R. G. Fowcett (1)
K. M. Siegel (1)

Cornell Aeronautical Laboratory
Buffalo, N. Y.
Dr. W. A. Flood (1)

Physical Science Laboratory
New Mexico College of A & MA
State College, N. M.
Dr. G. W. Cardiner (1)

Office of Naval Research
Washington 25, D. C.
Electronics Branch (1)

Raytheon Manufacturing Co.
Missile and Radar Division
P.O. Box 398
Bedford, Mas.
Mrs. Isabell Britton, Librarian (1)
Via Inspector of Naval Material
Bldg. 21 South Boston Annex
Boston Naval Shipyard
P.O. Box 2276
Boston 10, Mass.

Hughes Aircraft Co.
Florence Avenue at Teal Street
Culver City, California
Mrs. Audrey Diver (1)
Via Air Force Plant Representative
WEAPD
Hughes Aircraft Co.
Culver City, California

National Science Foundation
Washington 25, D. C.
Engineering Program (1)

Sandia Corporation
Sandia Base, Albuquerque, New Mexico
Mr. G. A. Fowler (1)
Mr. C. H. Bidwell (1)
Mr. G. W. Rodgers (1)
Mr. J. R. Ames (1)

Naval Research Laboratory
Washington 25, D. C.
Mr. D. L. Kingwalt (1)
Library (1)

Armed Services Tech. Information Agency (4)
Document Service Center
Knott Building
Dayton 2, Ohio

UNCLASSIFIED